Repeated loss of function at HD mating-type genes and of recombination suppression without mating-type locus linkage in anther-smut fungi

Elise A. Lucotte[1]§, Paul Jay[1], Quentin Rougemont[1], Loreleï Boyer[1], Amandine Cornille[2], Alodie Snirc[1], Amandine Labat[1], Elizabeth Chahine[1], Marine Duhamel[1], Jacob Gendelman[3], Wen-Juan Ma[3,4], Roxanne Kaaren Hayes[5], Michael H. Perlin[5], Michael E. Hood[3]*, Ricardo C. Rodríguez de la Vega[1]*, Tatiana Giraud[1]*§

* These authors co-supervised the study

[1] Ecologie Systematique et Evolution, CNRS, Université Paris-Saclay, AgroParisTech, 91198 Gif-sur-Yvette, France

[2] Université Paris-Saclay, INRAE, CNRS, AgroParisTech, GQE - Le Moulon, 91190 Gif-sur-Yvette, France

[3] Department of Biology, Amherst College, 01002-5000 Amherst, Massachusetts, United State of America.

[4] Department of Biology, Research group of Ecology, Evolution and Genetics, Vrije Universiteit Brussel, Brussels, Belgium

[5]Department of Biology, Program on Disease Evolution, University of Louisville, Louisville, KY 40292, USA

§ Corresponding authors:

Tatiana Giraud tatiana.giraud@universite-paris-saclay.fr

Elise Lucotte elise.lucotte@@universite-paris-saclay.fr

IDEEV, Bâtiment 680, 12 route RD128, 91190 Gif-sur-Yvette, France

phone: +33 1 69 15 56 69 fax: +33 1 69 15 46 97

Keywords: mating-type chromosomes, recombination suppression, fungi, sex chromosomes, mating-type loci, basidiomycota, evolutionary strata, *Dianthus,* sheltering hypothesis, stepwise recombination suppression

ABSTRACT

A wide diversity of mating systems occur in nature, with frequent evolutionary transitions in mating-compatibility mechanisms. Basidiomycete fungi typically have two mating-type loci controlling mating compatibility, HD and PR, usually residing on different chromosomes. In *Microbotryum* anther-smut fungi, there have been repeated events of linkage between the two mating-type loci through chromosome fusions, leading to large non-recombining regions. By generating high-quality genome assemblies, we found that two sister *Microbotryum* species parasitizing *Dianthus* plants, *M. superbum* and *M. shykoffianum*, as well as the distantly related *M. scorzonarae*, have their HD and PR mating-type loci on different chromosomes, but with the PR mating-type chromosome fused with part of the ancestral HD chromosome. Furthermore, progressive extensions of recombination suppression have generated evolutionary strata. In all three species, rearrangements suggest the existence of a transient stage of HD-PR linkage by whole chromosome fusion, and, unexpectedly, the HD genes lost their function. In *M. superbum*, multiple natural diploid strains were homozygous, and the disrupted HD2 gene was hardly expressed. Mating tests confirmed that a single genetic factor controlled mating compatibility (i.e. PR) and that haploid strains with identical HD alleles could mate and produce infectious hyphae. The HD genes have therefore lost their function in the control of mating compatibility in these *Microbotryum* species. While the loss of function of PR genes in mating compatibility has been reported in a few basidiomycete fungi, these are the first documented cases for the loss of mating-type determination by HD genes in heterothallic fungi. The control of mating compatibility by a single genetic factor is beneficial under selfing and can thus be achieved repeatedly, through evolutionary convergence in distant lineages, involving different genomic or similar pathways.

INTRODUCTION

Mating systems, corresponding to the degree of selfing/outcrossing, influence gene flow, genetic load and adaptability in natural populations[1,2,3,4,5,6,7]. A wide diversity of mating systems occur in nature, controlled by mating compatibility systems (e.g. separate sexes or mating types), with frequent evolutionary transitions between these systems[5,8,9,10,11]. In many animals and dioecious plants, different sexes are determined by sex chromosomes[12]. In hermaphrodite plants, mating compatibility is often controlled by a self-incompatibility locus, which prevents mating between identical alleles at this locus[13]. In fungi with mating types, gamete compatibility is controlled at the haploid stage, where only cells with different mating types can successfully mate[14,15], mating types being determined by one or two loci[16], the systems being then called uni- and bifactorial, respectively. There have been multiple transitions in fungi for changes in the number of loci controlling mating types, between one, two or even none, i.e., lack of discrimination for mating[8,15].

Recombination is typically suppressed at loci determining sexes and mating types, which ensures proper function in these complex phenotypes. Recombination suppression has furthermore often extended stepwise outward from these mating-compatibility loci in plants, animals and fungi[17,18,19,20,21,22,23,24], and the reason why is still debated[23,25]. It has long been accepted that recombination suppression extended on sex chromosomes because it was beneficial to link sexually antagonistic genes (i.e., with an allele being beneficial in only one sex) to the sex-determining locus[26]. However, little evidence could be found in favor of this hypothesis[27], and it cannot explain the stepwise extension of recombination suppression on fungal mating-type chromosomes, as they lack sexual antagonism and other kinds of antagonistic selection[17,23,28].

Other hypotheses have therefore been developed, in order to account for the ubiquity of stepwise extension of recombination suppression on sex-related chromosomes: the neutral accumulation of sequence divergence proximal to the mating-compatibility locus that would reduce recombination rates[29], the spread of transposable elements adjacent to the non-recombining mating-compatibility locus, together with their epigenetic marks[30], or the selection of non-recombining fragments carrying fewer deleterious mutations than the population average while having their load sheltered by a permanently heterozygous allele[31-33].

Following recombination suppression, Muller's ratchet and Hill-Robertson effect[34,35] lead to genomic degeneration, in terms of gene losses, weaker gene expression, lower frequencies of optimal codons, and transposable element accumulation[36,37,38,39,40,41]. Rearrangements also rapidly accumulate[17,18,42], so that recombination can be challenging to restore after the non-recombining fragments have become highly degenerated[31,33].

Basidiomycete fungi typically have two mating-type loci controlling mating compatibility[16]: the PR locus, controlling pre-mating fusion with pheromone and pheromone receptor genes, and the HD locus, controlling post-mating dikaryotic growth with two homeodomain genes whose products heterodimerize to form an active transcription factor[43]. These two loci are usually on different chromosomes and may harbor multiple alleles. Some basidiomycetes in contrast are unifactorial, i.e. with a single segregating unit controlling mating type, which is caused most often by HD-PR linkage, as in the crop pathogen *Ustilago hordei*[44] and human pathogens *Malassezia spp*[45,46], or more rarely by the loss of mating-compatibility role by the PR locus, as in the mushrooms *Coprinellus disseminatus*[47] and *Volvariella volvacea*[48]. A loss of mating-compatibility role by the HD locus has only been observed so far in experimental mutants with their two HD genes fused[49].

Microbotryum fungi (Basidiomycota) are plant-castrating pathogens, producing their spores in the anthers of diseased plants and therefore called anther-smut fungi. Most *Microbotryum* species specialized on one or a few host plants[50,51,52,53]. *Microbotryum* fungi are model organisms in as diverse fields as ecology, disease transmission, host specialization and reproductive isolation evolution, host-pathogen costructure, mating system and sex-related chromosome evolution[51,53,54,55,56,57,58,59,60,61,62]. *Microbotryum* fungi mostly undergo selfing via intra-tetrad mating[58,63,64], in which case carrying a single segregating mating-type locus is advantageous because it maximizes the odds of gamete compatibility[17]. *Microbotryum* fungi have in fact repeatedly evolved HD-PR linkage, with at least nine events of chromosomal rearrangements and recombination suppression between the two mating-type loci[17,18,39,41]. In addition, two non-sister *Microbotryum* species still have their mating-type loci on different chromosomes although each is linked to its centromere, resulting in the same odds of gamete compatibility as HD-PR linkage under intra-tetrad selfing[41,65]. Recombination suppression extended stepwise beyond mating-type loci in several lineages, forming evolutionary strata, i.e. fragments displaying decreasing differentiation with increasing distance to mating-type loci along the ancestral gene order[17,18,41].

121 The non-recombining regions on both mating-type chromosomes in *Microbotryum* fungi
122 display signs of genomic degeneration, as neither ever recombines. For example,
123 polymorphism is common for haploid sporidia of one or the two mating types failing to grow
124 *in vitro* in some *Microbotryum* species, likely due to deleterious mutations linked to mating-
125 type loci[58,66-68]. Indeed, with time since recombination suppression, these mating-type
126 chromosomes accumulate transposable elements, non-synonymous mutations, gene losses,
127 rearrangements and non-optimal codons [18,39,40,42,69]. Transposable elements accumulate rapidly
128 following recombination suppression, and some specific transposable element families
129 expanded preferentially on *Microbotryum* mating-type chromosomes, such as *Helitrons* and
130 *Copia/Ty3* elements[69,70]. These patterns are especially pronounced in species with linked HD
131 and PR loci and extensive suppression of recombination, in contrast to the genomes retaining
132 the ancestral state of unlinked mating types, that exhibit lesser severity of degenerative
133 processes[18,39,40,42,69].

134 Surveys of the diversity within *Microbotryum* fungi continue to yield novel insights, and
135 preliminary analyses suggested that the species parasitizing *Dianthus* plant species carried
136 unlinked HD and PR loci, yet displaying very high transposable element content compared to
137 other *Microbotryum* species[70]. Using two *Microbotryum* species on *Dianthus*, our aim was
138 therefore to characterize the mating-type chromosomes of these species, elucidate whether the
139 mating-type loci display localized recombination suppression, and if so, whether the mating-
140 type loci were linked together or to their respective centromeres. We found in both species a
141 large non-recombining mating-type chromosome issued from the fusion of the entire ancestral
142 PR chromosome and a part of the ancestral HD chromosome but, surprisingly, not HD locus
143 itself. Genome comparison indicated that the translocation occurred via a transient stage of
144 whole chromosome fusion, a few rearrangements and then separation of a part of the HD
145 chromosome arm. Remarkably, homozygosity was observed at the HD genes in natural
146 populations, indicating that they were not involved anymore in mating-type determination, and
147 one of the HD2 alleles appeared disrupted in *M. superbum*. This novel observation among
148 basidiomycete fungi was also found in a distant congeneric species, *M. scorzonerae*, with
149 unlinked PR and HD loci, but homozygosity and non-functionalization of HD genes, and
150 rearrangements between ancestral HD and PR chromosomes. These results demonstrate the
151 potential for genetic innovation in compatibility systems that directly influence how mating
152 system variation is achieved in nature. In addition, we found multiple evolutionary strata in the

153 three species, i.e., young extensions of recombination suppression on the mating-type
154 chromosomes.

155

156 **RESULTS**

157 **A large non-recombining PR chromosome including an arm of the ancestral HD**
158 **chromosome but not the HD genes**

159 We obtained high-quality genome assemblies from one strain from each of two *Microbotryum*
160 species parasitizing *Dianthus* plants: *M. superbum* (aka MvDsp2[52], strain 1065) and *M.*
161 *shykoffianum* (aka MvDsp1[52], strain c212). The phylogenetic tree based on 2,391 single-copy
162 orthologs representing 5.2 mb of nucleotide sequences placed them as sister species as expected
163 (Figure 1). In all four haploid genomes, the PR and HD genes were found on different contigs
164 (Figures 2 and S1-3) and with telomeric repeats identified on almost all of these mating-type
165 contig edges (Figure S4-6), showing that the two mating-type loci are located on different
166 chromosomes. We compared these mating-type chromosomes to those of *M. lagerheimii*,
167 inferred to be a good proxy for the ancestral gene order of *Microbotryum* mating-type
168 chromosomes[17,41]. We found the PR gene to be located in both *M. superbum* and *M.*
169 *shykoffianum* on a chromosome corresponding to the fusion of the ancestral PR chromosome
170 and a large part of the ancestral HD chromosome. The remaining part of the ancestral HD
171 chromosome, carrying the HD gene, was found on a separate chromosome (Figures 2 and S1-
172 4). This new PR chromosome was non-recombining across most of its length, as it was widely
173 rearranged between species and between a_1 and a_2 chromosomes in both *M. superbum* and *M.*
174 *shykoffianum* (Figures 2 and S1-5). Only small regions were collinear at both edges of the PR
175 chromosome, corresponding to recombining pseudo-autosomal regions (PAR, Figures S4-S5).
176 The centromere was identified within the non-recombining region and telomeres at the edges
177 of the new PR and HD chromosomes (Figures S4-S5). The separate chromosome carrying the
178 HD genes was very small in both species, and collinear between the two mating types as well
179 as between species (Figures 3 and S1-5), suggesting ongoing recombination.

180 In both *M. superbum* and *M. shykoffianum*, a few genes present on the HD chromosome part
181 carrying the HD genes in *M. lagerheimii* were however found in the non-recombining region
182 of the PR chromosome, and conversely (genes colored in green in Figures 3-4 and S4). This
183 indicates an ancient fusion between the whole PR and HD chromosomes, followed by a few
184 genomic rearrangements, before an excision of a part of the ancestral short HD chromosome
185 arm (Figure 3). Such an excision may have occurred in a single step or by chromosome fissions

186 followed by a new fusion. Some of the genes that were found reshuffled between the ancestral
187 PR and HD chromosomes were different between *M. superbum* and *M. shykoffianum*, which
188 may suggest that the fission of the current small HD chromosome occurred independently in
189 the two species, after their speciation.

190 Nucleotide polymorphism data further indicated that the PR chromosome was mostly non-
191 recombining and that the HD genes were not linked to the PR gene in the *Microbotrum* fungi
192 parasitizing *Dianthus* plants. Using SNPs on 149 Illumina genomes collected on various
193 *Dianthus* plants in western Europe, high levels of LD were found across most of the PR
194 chromosome, while LD levels were much lower between HD and PR contigs (Figure S7). The
195 LD values within the HD chromosome, as well as against the PR chromosome, were a bit
196 higher than those within autosomes, but were similar as those between the HD chromosomes
197 and autosomes, thus not indicating linkage.

198 The high per-gene synonymous divergence (d_S) between alleles on the a_1 and a_2 mating-type
199 chromosomes (Figures 4-5) further confirmed the lack of recombination along most of the PR
200 chromosome, while the HD chromosome appeared recombining. Indeed, because selfing in
201 *Microbotryum* anther-smut fungi yields high homozygosity levels, recombining region shows
202 zero d_S values between alleles in recombining regions such as autosomes, pseudo-autosomal
203 regions of the PR chromosome and in the HD chromosome (Figures 4-5). In contrast, the
204 rearranged region of the PR chromosome displayed high d_S values in both *M. superbum* and *M.*
205 *shykoffianum* (Figures 4-5). Following previous studies on *Microbotryum* fungi, the region
206 initially linking the PR and HD genes was called the black stratum (Figures 4-5), although this
207 stratum does not link the PR and HD mating-type loci any more due to the proposed fission of
208 the HD-containing chromosome arm (Figure 3). This black stratum evolved before the
209 divergence of the *M. superbum* and *M. shykoffianum* lineages, as 73% of the genes showed full
210 trans-specific polymorphism between these two lineages (Figure 6): the alleles clustered
211 according to a_1 or a_2 mating type rather than species in gene genealogies, indicating
212 recombination suppression before speciation. We found footprints of previously inferred
213 evolutionary strata (i.e. the blue, purple and orange strata; Figures 4-5), that were shown to
214 have evolved around the HD and PR genes ancestrally in the *Microbotryum* clade[17,18,23].

215 In the *M. shykoffianum* genome, the HD chromosome in the a_2 assembly was much shorter than
216 in the a_1 assembly, while still carrying the HD gene (Figure S4-5). The mapping of diploid
217 reads on the a_1 plus a_2 genome assemblies showed double coverage in the missing regions of

218 the HD chromosome, indicating the collapse of the two homologous chromosomes in the
219 corresponding regions in the a_1 assembly (Figure S8). The coverage was however not doubled
220 in a small region at the edge of one pseudo-autosomal region, and the corresponding genomic
221 region was not found in the a_2 genome assembly, suggesting that this small region may be
222 genuinely missing in the a_2 genome (Figure S8).
223
224 **Loss-of-function in mating-type determination of HD genes and lack of PR-HD linkage**
225 **established by segregation analyses**
226 The alleles of the two tightly-linked HD genes (HD1 and HD2) appeared functional in the two
227 haploid genomes of *M. shykoffianum* and in the a_1 genome of *M. superbum*, but not in the a_2
228 genome of *M. superbum*. The HD2 gene indeed appeared separated into two different protein
229 coding sequences (CDS) in the a_2 genome in *M. superbum,* with an early stop codon and a new
230 start codon (Figure 7). One of the two novel CDS appeared expressed during mating conditions,
231 but not *in planta*, and we detected no expression of the HD2 gene in mating conditions or
232 when cultured as haploid. This may be because the strain is homozygous or because the a1
233 allele of HD2 is not expressed. In contrast, in *M. lychnidis-dioicae* (with non-recombining
234 mating-type chromosomes) and *M. intermedium* (with almost fully recombining mating-type
235 chromosomes) both HD genes are upregulated under mating or *in planta* conditions (Figure 7).
236 Analyses of non-synonymous substitution proportions based on gene genealogies with all
237 available species (Figure 1) indicated significant positive selection in the two new CDS,
238 suggesting neofunctionalization (significant test for selection intensification: K = 22.64; p =
239 0.001, LR = 11.37).

240 Mating tests confirmed that HD genes have lost their mating-type determination function in *M.*
241 *superbum*. We isolated the four meiotic products of 12 full tetrads from a strain collected on
242 *D. pavonius* in the same site as the reference strain. *Microbotryum* produces linear tetrads
243 allowing assessment of first versus second division segregation[58,71]. We tested whether each of
244 these haploid cell lineages would mate with tester haploid strains from one of the tetrads that
245 carried a_1 or a_2 PR alleles, respectively, as determined by PCR[72]. The typical situation in
246 heterothallic basidiomycete fungi is that i) only haploid cells carrying different PR alleles can
247 fuse and ii) only haploid cells carrying different HD alleles can produce hyphae when mated.
248 In all 12 tetrads but one, two of the four meiotic products conjugated with the a_1 tester and the
249 other half with the a_2 testers, as expected, with PR alleles segregating at the first meiotic
250 division, consistent with linkage of the PR gene to its centromere shown above. Supporting the

251 view that the HD genes no longer have a role in mating-type determination, all meiotic products
252 compatible for conjugation with a given mating tester also produced hyphae. If HD genes were
253 still involved in mating-type determination, only half of conjugated pairing would produce
254 hyphae due to independent segregation/assortment of PR and HD mating type loci inferred
255 from genomic assemblies.

256 Additionally, PCR tests confirmed that the 12 meiotic tetrads analysed in *M. superbum* resulted
257 from a field-collected diploid parental genotype that contained identical HD alleles, which
258 indicates the lack of mating-type role of HD genes. We indeed designed primers that would
259 specifically amplify only the allele present in the a_1 or a_2 genome of the *M. superbum* 1065
260 strain (Table S1). The primers for the HD1 and HD2 genes gave PCR products only with the
261 primer pair designed to amplify the alleles in the a_2 genome of the *M. superbum* 1065 strain,
262 and in all four meiotic products of all tetrads, indicating homozygosity of the diploid parent.
263 Sanger sequencing of the amplicons confirmed that all meiotic products were identical at the
264 HD genes. Therefore, heterozygosity at the HD genes was not required any more in these
265 strains for successful mating and hyphae production. We also inoculated *D. chinesis* in the
266 greenhouse and showed these homozygous pairs could cause disease (5 out of 24 inoculated
267 plants, as typical under inoculations). In one tetrad, two meiotic products produced hyphae
268 alone without any tester strains and the PCR indicated that these sporidia contained the two PR
269 alleles, likely following abnormal meiotic segregation (i.e. non-disjunction), as previously
270 reported in *Microbotryum* fungi (back then called *Ustilago violacea*)[73]. This sporidial line
271 however did not produce disease upon plant inoculation.

272 We further pulled out two tetrads from each of six additional field-collected *M. superbum*
273 strains. Two strains were homozygous for the HD genes, confirming that mating can occur
274 between cells with identical HD alleles; the other strains were heterozygous. Across tetrads,
275 the PR alleles were not always associated to the same HD alleles, which confirms that the HD
276 and PR loci are unlinked in this species (Table S2).

277 The HD1 and HD2 coding sequences in *M. shykoffianum* c212 were not disrupted but were
278 100% identical between the a_1 and a_2 genomes, while the PR alleles showed high differentiation
279 and trans-specific polymorphism as expected. This reinforces the view that the HD genes can
280 be homozygous in *Microbotryum* strains from *Dianthus* species, and that, therefore, HD genes
281 are not involved anymore in mating-type determination.

282 Polymorphism analysis of the HD genes based on Illumina sequencing confirmed that they
283 could be homozygous in natural strains. We used SNPs called in the 149 Illumina genomes
284 against the a_1 *M. superbum* reference plus the HD and PR chromosomes from the a_2 genome.
285 The genomes were obtained by spreading diploid teliospores on culture medium, where they
286 undergo meiosis and haploid meiosis product multiply. In 23 strains, we found only significant
287 mapping on the a_1 PR chromosome and in 14 strains only on the a_2 PR chromosome. This is
288 likely due to haplo-lethal alleles on the PR chromosome, with gene disruptions that are lethal
289 at the haploid stage due to degeneration following recombination suppression, preventing
290 growth of haploid sporidia on our culture plates, as identified in several *Microbotryum*
291 species[58,66,68]. Among the 62 strains for which we were confident that they carried the two PR
292 chromosomes (and therefore confidently sequenced as diploids), 42 exhibited polymorphism
293 at the HD genes in SNP data, indicating heterozygosity, while 20 showed no polymorphism at
294 the HD genes. These findings confirm that heterozygosity at HD genes is no longer required
295 for mating compatibility or completion of the life cycle. The SNP analysis further indicated a
296 high selfing rate in these fungi: the F_{IS} mode on autosomes was at 0.83, corresponding to a
297 selfing rate of ca s=0.91 using the formula $s=2F_{IS}/(1+F_{IS})$.

298 **Loss of function of HD genes in *M. scorzonerae* and genomic rearrangements**

299 We also identified a loss of HD gene function and homozygosity of field-collected samples in
300 a distant species, *M. scorzonerae* (Figure 1). Oxford Nanopore sequencing of two haploid
301 genomes isolated from the same meiotic tetrad and with opposite PR alleles, revealed identical
302 sequences for both HD1 and HD2 genes. We performed mating tests between meiotic products
303 of 22 tetrads, which again indicated compatibility segregating a single mating-type locus: when
304 cells were compatible for PR-determined conjugation, they also produced hyphae in 100% of
305 the cases.

306 The HD1 sequences from the sequenced *M. scorzonerae* a_1 and a_2 haploid genomes appeared
307 to have an uninterrupted coding sequence. The HD2 coding sequences displayed a 19 bp gap
308 inducing a frameshift mutation in the coding region and a stop codon which would truncate the
309 gene to 120 amino-acids instead of 487 amino-acids in *M. lagerheimii*. Using PCR
310 amplification and Sanger sequencing, we confirmed that the frameshift is present in all the
311 isolated cultures, as well as in the *M. scorzonerae* sample not used to produce haploid cultures.
312 As in *M. superbum*, the analysis of 22 tetrads indicated that a single genetic factor controlled
313 mating type in *M. scorzonerae*.

314 The a_1 and a_2 genome for *M. scorzonerae* did not assemble as well as for *M. superbum* and *M.*
315 *shykoffianum.* Nevertheless, we identified two contigs in the a_1 *M. scorzonerae* assembly that
316 carried regions corresponding to the ancestral PR and HD chromosomes, and also parts of *M.*
317 *lagerheimii* autosomes, indicating that mating-type chromosome fusion occurred, and also with
318 ancestral autosomes (Figure S9A). The contigs carrying parts of the ancestral PR and HD
319 chromosomes were nevertheless collinear between the a_1 and a_2 *M. scorzonerae* genomes,
320 indicating ongoing recombination, with the exception of a relatively small non-recombining
321 region around the PR locus (Figure S9B). The HD and PR genes were not in the same contigs.
322 This suggests that there was a transient stage, as in *M. superbum* and *M. shykoffianum,* where
323 the HD and PR genes were linked by chromosomal fusion of ancestral HD and PR
324 chromosomes, as well as autosomes, followed by chromosomal rearrangements and subsequent
325 loss-of-function of HD genes in mating-type determination. We could not detect telomeres
326 however in any of these contigs.

327

328 **Progressive recombination suppression in the mating-type chromosome: evolutionary**
329 **strata**

330 We found evidence of four young evolutionary strata specific to the mating-type chromosome
331 of *M. superbum* or of *M. shykoffianum,* therefore resulting from recent extensions of
332 recombination cessation. Indeed, when plotting the per-gene synonymous divergence between
333 mating-type chromosomes in *M. superbum* 1065 along the ancestral gene order (taking *M.*
334 *lagerheimii* gene order as a proxy[18,41]), we found a region with significantly lower d_S values at
335 the edge of the non-recombining region, while significantly different from zero (Figures 4 and
336 S10). We called this region the "turquoise" evolutionary stratum following previous color
337 names given to young evolutionary strata in *Microbotryum* fungi. This turquoise stratum is
338 currently situated within the non-recombining region of the PR mating-type chromosome
339 (Figures S4-5 and S11) while remaining still much less rearranged than the rest of the non-
340 recombining region, as expected for a young evolutionary stratum. This very same turquoise
341 stratum had in contrast zero d_S values in *M. shykoffianum* and has remained in the pseudo-
342 autosomal region (Figures 5 and S4-S5). An additional evidence for the evolution of the
343 turquoise stratum post-dating speciation between *M. shykoffianum* and *M. superbum* is the lack
344 of trans-specific polymorphism (Figure 6). A single gene displayed full trans-specific
345 polymorphism in the turquoise stratum and it was situated just at the limit with the black
346 stratum, and it may actually belong to the black stratum. Altogether, these findings show that

347 the turquoise stratum has moved into the non-recombining region in *M. superbum* after its
348 divergence from *M. shykoffianum*, thus constituting a young evolutionary stratum (Figure 3).

349 We found footprints of another young evolutionary stratum in *M. superbum*, on the other side
350 of the PR mating-type chromosome in the ancestral chromosomal arrangement. The d_S plot
351 indeed showed high d_S values in the left edge of the PR chromosome (Figure 4), in the region
352 that we called "ruby" (Figure 5).

353 A changepoint analysis confirmed the inference of distinct evolutionary strata in *M. superbum*,
354 with the turquoise and ruby strata showing significantly lower mean d_S value than the black
355 stratum, with discrete changes in mean values (Figure 4). The changepoint analysis even
356 indicated that the ruby stratum was divided into two distinct sub-strata of different ages, that
357 we called the "dark" and "light' ruby strata, with significant different mean d_S values and
358 different locations: the dark ruby stratum was rearranged, while the light ruby stratum was still
359 at the edge of the chromosome (Figures 4 and S4). The black, turquoise, light and dark ruby
360 strata in fact had significant different d_S mean values than their nearby strata (Figure S10).

361 The dark ruby stratum was only partly present in *M. shykoffianum* (Figure 5), suggesting either
362 an independent origin in the two lineages or an ancestral stratum that would have partly restored
363 recombination in *M. shykoffianum.* This latter hypothesis is supported by the lack of detected
364 change-point in *M. superbum* within the dark ruby stratum, indicating it evolved in a single
365 step (Figure 4). Moreover, trans-specific polymorphism was found for the genes from the right
366 part of dark ruby stratum that have high d_S values in the two species (Figures 4-5).

367 In *M. scorzonareae,* genes around the PR locus were highly rearranged between mating-type
368 chromosomes and compared to the *M. lagerheimii* gene order (Fig S9), indicating ancient
369 recombination suppression, which was further supported by high d_S values (Fig S13). This non-
370 recombining region extended farther than the purple and orange strata shared among all
371 *Microbotryum* species, indicating an extension of recombination suppression specific to *M.*
372 *scorzonareae.* We called this extension the emerald stratum, and it encompassed not only a
373 part of the ancestral PR chromosome, but also a small fragment of the ancestral HD
374 chromosome, from the middle of the MC03B *M. lagerheimii* contig: this fragment indeed
375 displays elevated d_S values in *M. scorzonareae* (Fig S13) and is currently located near the PR
376 locus because of the inter-chromosomal rearrangements (Fig S9). In addition, we detected
377 footprints of a younger specific evolutionary stratum, called quartz, with very low d_S values
378 (Fig S13), being collinear between a_1 and a_2 PR mating-type chromosomes but having moved

379 from the PAR to the middle of the non-recombining region in the a_2 PR chromosome (Fig S9).
380 The non-zero d_S values extend a bit farther towards the PAR than the translocated fragment,
381 suggesting that the quartz stratum may be larger than this translocated fragment.
382 We used the divergence time between M. lychnidis-dioicae and M. silenes-dioicae as a
383 calibration point (0.42 million years[74]) to estimate the age in million years (MY) of the various
384 evolutionary strata and their confidence intervals (CI), based on autosomal single-copy genes.
385 We estimated the following ages: 1.55 MY for the black stratum (CI 1.21-1.92), 1.25 MY for
386 the dark ruby stratum (CI 0.75-2.23), 0.28 MY for the light ruby stratum (CI 0.16-0.45), 1.61
387 MY for the emerald stratum (CI 1.03-2.33) and 0.06 MY for the quartz stratum (CI 0-0.16).

388

389

390 **Degeneration of the PR mating-type chromosomes**

391 In both *M. superbum* and *M. shykoffianum*, the PR mating-type chromosome shows chaos of
392 rearrangements between the a_1 and a_2 genomes and in comparison to the ancestral gene order,
393 taking as proxy the *M. lagerheimii* PR chromosome (Figures 2, S1-S5). Similarly, expected of
394 non-recombining regions, the PR chromosome has also accumulated transposable elements
395 (TEs), as seen by the much higher TE content in the a_1 and a_2 PR chromosomes in *M. superbum*
396 (65% and 67% of bp, respectively) compared to its autosomes (mean 35% of bp) (Figure 8).
397 Some TE families seem to have preferentially expanded, i.e. *Copia*, Ty3 (*Gypsy)* and *Helitrons*
398 (Figure 8). As a result, the PR chromosome has become much larger than its ancestral
399 recombining state (Figure 8, 12,930,922 vs 942,259 bp). In contrast, the HD chromosome did
400 not have an TE load (mean 36% of bp, Figures), in agreement with the inference of continued
401 recombination in this chromosome.

402

403 **DISCUSSION**

404 A wide variety of breeding systems have been reported across fungi, including universal
405 haploid compatibility, a single mating-type locus or two mating-type loci[8,14]. The role of PR
406 and HD genes in mating-type determination and their location on different chromosomes is
407 ancestral in basidiomycetes, corresponding to a bifactorial system, i.e., with two different
408 mating-type loci. Having two distinct loci controlling mating compatibility can favor
409 outcrossing, while having a single mating-type locus is advantageous under selfing: one
410 mating-type locus yields 50% compatibility among gametes of a given diploid individual
411 versus only 25% with two mating-type loci[56]. There have been multiple independent transitions

412 across the Basidiomycota from bifactorial to unifactorial systems, i.e., with a single genetic
413 locus determining mating compatibility. Unifactorial compatibility can occur through two main
414 pathways: linkage of PR and HD loci or the loss of function at one of the mating type loci[8].
415 Linkage between mating-type loci has been observed in *Ustilago hordei*[44] and multiple times
416 independently in the *Malassezia*[45,46] and *Microbotryum*[18,41] clades, as well as in other
417 basidiomycetes[8,75-78].

418 Loss-of-function at one of the mating-type loci, specifically at the PR locus, has also been
419 observed in several basidiomycete fungi, including *Pholiota nameko*[79], *Coprinellus*
420 *disseminatus*[47], and others[8]. To the best of our knowledge, this study in *Microbotryum* is the
421 first known case of functional loss at the HD locus in natural populations of heterothallic
422 basidiomycete fungi. This shows that unifactoriality, i.e. the segregation of only two mating
423 types in progenies, can be convergently acquired through a variety of different genomic
424 pathways in selfing fungi, for which it is beneficial. Furthermore, we found convergent events
425 of HD gene loss-of-function after a transient HD-PR chromosome fusion, in two very distantly
426 related anther-smut fungi. Altogether, this sheds new light on the power of selection and on the
427 repeatability of evolution, and shows that similar phenotypes can be achieved repeatedly, via
428 similar or different genomic mechanisms.

429 In addition, finding this example of an HD loss-of-function has important implications for our
430 understanding of the sexual cycle and gene functions in basidiomycete fungi. The two tightly-
431 linked genes of the HD locus, HD1 and HD2, are indeed thought to be essential for dikaryotic
432 growth, as they heterodimerize to activate the dikaryotic growth and can only do so between
433 different allelic forms at the two genes (using b_1 and b_2 to denote different alleles and where
434 haploid genomes typically carry either HD1 b_1 with HD2 b_1 or HD1 b_2 with HD2 b_2, dikaryotic
435 growth is triggered by HD1 b_1 with HD2 b_2 or HD1 b_2 with HD2 b_1). Uniting the two
436 compatible variants in a haploid genome could allow dikaryotic growth without the need to
437 mate with a different haplotype, as shown experimentally with a mutant carrying a chimeric
438 homeodomain protein in the mushroom *Coprinus cinereus*[49]. The need for HD heterodimers
439 may be bypassed for dikaryotic growth, as shown in the invasive Californian death cap
440 mushroom, *Amanita phalloides,* that can mate as a haploid homothallic, despite the two HD
441 genes in haploid genomes being unable to form a heterodimer[80]. Another possibility may be as
442 in the homothallic basidiomycete yeast *Cystofilobasidium capitatum*, in which the HD1/HD2
443 heterodimer has likely been replaced by a HD2 homodimer[81]. This hypothesis would explain
444 the positive selection detected on the new HD coding sequences.

445 Given the loss of the HD role in mating-type determination, it was intriguing to discover that
446 the PR chromosome had incorporated a fragment of the ancestral HD chromosome and was
447 non-recombining throughout most of its length. Indeed, the large non-recombining regions in
448 *Microbotryum* fungi are generally partly due to the linkage of HD and PR genes, even if further
449 extension of the non-recombining region has repeatedly evolved[18,41]. In the *Microbotryum*
450 species parasitizing *Dianthus* and *Scorzonareae* plants analysed here, a transient stage seems
451 to have occurred, with HD-PR linkage by fusion of the whole PR and HD ancestral
452 chromosomes, followed by a few rearrangements and then excision of a part of the ancestral
453 HD chromosome, likely once HD has lost its function. This hypothesis is supported by our
454 finding of genes belonging to the ancestral HD-containing chromosome arm being now located
455 on the PR chromosome in each of *M. superbum* and *M. shykoffianum.* Reversion to unlinked
456 mating-type chromosomes has been suggested in *Malassezia*-related fungi[46], but both mating-
457 type loci kept their functions, such that reversion was likely driven by changes in mating
458 systems. Here the chromosome fission may have followed the loss of function of the HD genes,
459 as this loss of function would offset the benefit of HD-PR linkage. Alternatively, the fission
460 may have occurred first, followed by the loss of function of the HD genes, selected for
461 unifactoriality, being advantageous under selfing.

462 This study also provided further support for the existence of three young, species-specific
463 evolutionary strata associated with the mating type loci in *Microbotryum* fungi. *M. superbum*,
464 *M. shykoffianum* and *M. scorzonareae* displayed high differentiation between mating-type
465 chromosomes and rearrangements within the non-recombining region, but lower differentiation
466 and lower levels of gene order reshuffling in young evolutionary strata than the rest of the non-
467 recombining region. The evolutionary cause for such stepwise and repeated recombination
468 suppression events may be a combination of selection for less genetic load in non-recombining
469 fragments and deleterious-mutation sheltering[31]. Indeed, if a non-recombining fragment traps
470 fewer recessive deleterious alleles than average in the population, this fragment will have a
471 selective advantage, but can only become fixed if it also captures a permanently heterozygous
472 allele that will shelter its few recessive deleterious mutations when it becomes frequent enough
473 to often be homozygous in populations[31]. The only other hypothesis that can explain such
474 repeated evolutionary strata on fungal mating-type chromosomes is a neutral fixation of
475 inversions or genetic differences impairing recombination[29], but this does not explain the
476 observed association between dikaryotic life cycle and evolutionary strata in fungi[33]. The
477 proximal mechanism of recombination suppression may be the observed movements of

478 fragments from the pseudoautosomal region into the non-recombining region, forming the
479 young strata, as previously reported for the red stratum in *M. lychnidis-dioicae*[17]. However,
480 such movements can also be a consequence, rather than a cause, of recombination suppression.

481 As expected, the older part of the non-recombining region on the PR mating-type chromosome
482 shows signs of degeneration, with chaos of rearrangements and high TE load. Some TE
483 families have preferentially expanded, i.e. *Copia*, Ty3 (*Gypsy)* and *Helitrons*, corresponding
484 to the same families that repeatedly expanded in mating-type chromosomes of other
485 *Microbotryum* species[69].

486 Given such accumulated load that results from mutational degeneration, it has been suggested
487 that reversion towards recombination could be selected for under the lower-loaded-sheltering
488 hypothesis, unless dosage compensation evolves[32]. Our scenario actually proposes an early
489 reversion of recombination suppression along a part of the ancestral HD chromosome. The
490 chaos of rearrangements on both mating-type chromosomes in the oldest evolutionary strata,
491 however, reinforces the view that rearrangements accumulate following recombination
492 suppression such that it seems challenging to restore recombination when load has
493 accumulated[31,33]. Recombination restoration would be even more difficult if the proximal
494 mechanism of recombination suppression is the movement of pseudo-autosomal regions into
495 non-recombining regions, as observed for young evolutionary strata. Recombination
496 restoration would indeed then require the exact same movement back, with exactly the same
497 breakpoints, which seems highly implausible. Our findings suggest that recombination
498 restoration may occur when rearrangements are not too extensive, as evidenced by i) the
499 footprints of recombination suppression followed by chromosome separation and
500 recombination restoration in the HD chromosome arm, ii) the reversion of a part of the dark
501 ruby stratum to a recombining state in *M. shykoffianum.* However, recombination restoration
502 now seems impossible in the non-recombining region of the PR chromosome given the chaos
503 of rearrangements there in both mating-type chromosomes.

504 In conclusion, our study brings novel insights into the evolution of breeding systems and sex-
505 related chromosomes, reporting unprecedented cases of loss-of-function of HD mating-type
506 genes in fungi, and fusion of ancestral mating-type chromosomes without linkage of mating-
507 type genes. Our findings further reinforce the view that recombination suppression can extend
508 progressively in organisms without sexual antagonism.

509

510 # Material and methods

511 ## Study systems

512 *Microbotryum* fungi, parasitizing *Dianthus* and *Silene* species, castrate plants by producing
513 their spores in the anthers of host plants and aborting the ovaries. Diseased plants are
514 identifiable by dark-colored spore masses in their flowers. Most *Microbotryum* fungi are
515 specialized on a single host species and most host species harbor a single *Microbotryum* species,
516 especially in the *Silene* genus[51,52,53,82]. One exception is the clade of *Microbotryum* fungi
517 parasitizing wild carnation relatives in the pink family (*Dianthus* genus, Caryophyllaceae), in
518 which several closely-related and sympatric *Microbotryum* species parasitize multiple
519 *Dianthus* plant species, with host range overlapping to some extent[52,53,83,84] (Figure 1). Three
520 species have been formally described so far in this group[84], but they are challenging to
521 recognize based on their host plant or morphology. We therefore assigned strains to species
522 based on the published sequences of the gene barcodes used for describing the species (EF1-
523 alpha and beta-tubulin;[52,84]; see below). *Microbotryum scorzonerae* parasitizes flowers of
524 *Scorzonera humilis*, in the Asteraceae family[85]. Unlike other *Microbotryum*, *M. scorzonerae*
525 does not cause spore formation on anthers alone. It instead causes spore formation within the
526 entire floral head (Figure 1).

527 ## <u>Genomic analyses</u>

528 ### Strains, DNA extraction and species identification

529 We extracted DNA as previously described[17,18]. For the *Dianthus* strains, DNA sequencing
530 based on PacBio (Pacific Bioscience) HiFi long-read sequencing was performed at the
531 GenoToul sequencing facility (Toulouse, INRAE, France) in 2021. We isolated haploid
532 sporidia of opposite mating types from a single meiosis (tetrad) from the strain 1065, collected
533 in July 2011 on *Dianthus pavonius*, in Italy (coordinates 44.189, 7.688, near the Garelli
534 Refugium in the Alps) by Michael Hood, Janis Antonovics and Emme Bruns. Based on
535 preliminary analyses of SNPs, we also identified a strain belonging to another *Microbotryum*
536 species parasitizing *Dianthus* plants: strain C212 (CZ_D24), collected in 2016 on *Dianthus*
537 *carthusianorum*, in the Czech Republic, coordinates 49.639759, 14.201153 (Bohemia, The
538 Vltava river basin, to the north of Zduchovice) by Klara Koupilova. This later strain had been
539 cultivated on Petri dishes at the haploid stage after spreading diploid teliospores that each
540 underwent meiosis; we therefore sequenced a mixture of haploid sporidia resulting from

541 multiple meioses from a single diploid individual. The mixture is thus equivalent to a diploid
542 genome. Cultivation of sporidia was performed on PDA (potato dextrose agar)[86]. The samples
543 were collected in Italy, which is not a party of the Nagoya protocol, and in the Czech Republic,
544 which does not regulate access to its genetic resources in relation to the Nagoya Protocol. Using
545 the best BLAST hits of the EF1-alpha and beta-tubulin genes against the reference
546 sequences[52,84], we assigned the strain 1065 to *M. superbum* (aka MvDsp2) and the strain C212
547 to *M. shykoffianum* (aka MvDsp1)[52,84]. For the *M. scorzonarae* strain, obtained in 2018 from
548 Cefn Cribwr, Wales, by Julian Woodman, sporidia of opposite mating types were isolated from
549 a single meiosis (tetrad). Although a party to the Nagoya Protocol, the UK does not regulate
550 access to its genetic resources. From cultures on PDA, extracted haploid genomic DNA was
551 used to generate long-read sequences with MinION (Oxford Nanopore Technologies), and
552 short- read Illumina sequencing.

553 **RNAseq from *M. superbum* and *M. intermedium***

554 We generated RNAseq data for gene prediction and HD gene expression analysis. For
555 optimizing gene prediction, we sequenced RNA from one of the focal species, *M. superbum,*
556 and also from an outgroup to our studied *Microbotryum* species, *M. intermedium*. For *M.*
557 *intermedium,* we used the strain BM12-12.1 (the same strain as used previously for genome
558 sequencing[17,39]), under two different conditions: 1) haploid cells of a single PR mating type (a_1
559 or a_2) grown on nutrient medium (PDA) and then mixed in equal proportions of the two mating
560 types before RNA extraction ("H" condition), as well as additional replicates grown separately
561 on nutrient agar, whose transcriptomes were analyzed separately, and 2) mixtures of cells of
562 the two mating types under mating conditions ("M" condition), i.e. on water agar. Total RNA
563 was isolated from haploid *M. intermedium* cells using the Monarch® Total RNA Miniprep Kit
564 (New England Biolabs). For the nutrient medium condition, haploid strains (a_1 or a_2) were
565 streaked onto potato dextrose agar (PDA) and grown for 3-4 days at 22 °C. Cells were scraped,
566 suspended in DNA/RNA protection solution, disrupted mechanically in the presence of acid-
567 washed glass beads (0.5 mm dia), and then total RNA was extracted following the
568 manufacturer's protocol. For the mating condition, haploid a_1 and a_2 cultures were first grown
569 separately in yeast extract peptone dextrose (YPD) broth overnight. Cell density was measured
570 with a spectrophotometer. The concentration of each culture was adjusted to O.D.600 1.0.
571 Equal volumes of the two haploid cultures were mixed and plated on water agar. These plates
572 were incubated for four days at 14°C, after which wet mounts were prepared from each "mated"

573 plate to verify the presence of conjugation tubes, indicating active mating behavior. Cells were
574 scraped and then total RNA was isolated using the Qiagen RNeasy Plant Mini Kit. After total
575 RNA isolation, several quality control measures were taken. Concentration and purity were
576 assessed using a NanoDrop 2000 spectrophotometer (Thermo Scientific); 260/280 and 260/230
577 ratios>1.8 were considered satisfactory for RNAseq application. Additionally, cDNA was
578 prepared and used as a template for intron-spanning primers in PCR reactions to verify the lack
579 of genomic DNA contamination. Bioanalyzer analysis was completed to detect intact 18S and
580 23S RNA as a measure of overall RNA quality. After passing all quality control measurements,
581 RNA was sent for sequencing to CD Genomics (Shirley, NY, USA). Three replicates were
582 sequenced per condition and means across the three replicates were analyzed.

583 For *M. superbum,* we used another strain from the same *D. pavonius* population as the strain
584 1065 (coordinates 44.191, 7.685, near the Garelli Refugium in the Italian Alps) for RNASeq,
585 a_1 and a_2 haploid strains were used separately as well as pooled in mating experiments. For
586 extractions from haploid cells grown on PDA, we used the Zymo -----RNA Extraction Kit
587 (Zymo Research, Irvine, California). Prior to RNA extractions, each haploid fungal strain was
588 grown on two PDA Petri dishes at 28°C for 24 hours. Extractions were performed on fungal
589 cells from the two PDA Petri dishes for each haploid sample replicate. Fungal mating was
590 accomplished in the following steps. Haploid *M. superbum* a_1 and a_2 cells were grown on YPD
591 agar for four days prior to the mating assay. Haploid cells were then suspended in distilled and
592 autoclaved water before adjusting to 10^9 cells/mL. Suspended fungal cells were combined in
593 equal proportions before being spotted in 50 µl spots on water agar Petri dishes. Plates were
594 left to incubate at 13° Celsius for 48 hours. Resulting cells were visualized under a light
595 microscope to confirm the occurrence of mating via the formation of conjugation tubes between
596 cells. Under these conditions we typically observed about 30% of the cells engaged in mating.
597 Extractions using the Zymo RNA extraction kit were performed on mated fungal tissue that
598 was aggregated from the water agar petri dishes for each mated sample. RNAseq of three
599 biological replicates per condition (mated, haploid a_1 and haploid a_2) were performed by CD
600 Genomics (Shirley, New York).

601 Three *D. pavonius* plants infected with *M. superbum* were obtained from Emme Bruns at the
602 University of Maryland. For generating these diseased plants, seeds of *D. pavonius* were
603 collected from two populations in Aug 2016 in Italy (Duca coord. 44.1946327, 7.66067016
604 and Garelli coord. 44.189128, 7.688879), which is not a party of the Nagoya protocol. They

605 were reared in greenhouse conditions planted in Sept 2016, reared and crossed within
606 populations in 2017 to produce seeds at the University of Maryland. F1 seeds were planted and
607 inoculated in 2018 with a strain from the Duca population, and scored as diseased 2020. The
608 plants (DE 10B 3; HL-2 duca 1061; De 10A 8) were used for RNAseq production. Four
609 different flower bud size binspools were used in these analyses: 11-12 mm, 13-14 mm, 15-16
610 mm, and 18-20 mm. These represented different stages of both host and parasite development.
611 RNA extractions from plant tissue were performed using Qiagen -----RNA Extraction Kit.
612 Flower buds were harvested from plants that were maintained in a controlled growth chamber.
613 The number of flower buds used for each extraction was dependent on the size of the buds that
614 were collected. All extractions with flower buds that fell into the 11-12 mm bin category were
615 completed with at least two flower buds while extractions on buds in the 13-14 mm or larger
616 bin categories used one flower bud per reaction. In total we sent 9 samples from three plants
617 for RNAseq (CD Genomics).

618 **Expression of HD genes**

619 For the gene expression analysis on HD genes, we used only the conditions under which we
620 had multiple technical replicates and for which HD genes are expected to be expressed, i.e, the
621 three 11-12 mm *M. superbum* replicates obtained from the same plant and the three replicates
622 from each of the culture conditions (mated at 48 h and haploid cultures). Expression of HD
623 genes in *M. lychnidis-dioicae* and *M. intermedium* M. lychnidis-dioicae, or PDA, M.
624 intermedium, and for both under mating conditions at 48 h[39,76] was assessed as a control of
625 expectations for functional HD genes, in two or three replicates for each of three culture
626 conditions (haploid cultures of alternative mating types grown on water, *M. lychnidis-dioicae*,
627 or PDA, *M. intermedium*, and for both under mating conditions at 48 h[39,87]) and from infected
628 flowers at a late stage[88], see Table S3. To check whether HD genes were expressed, reads were
629 mapped with minimap2 2.26-r1175[89] with the -ax sr option, depth per base extracted with
630 samtools depth function[90], explored with jbrowse 2[91] and visualized with plotkaryotypeR[92].

631 **Genome assemblies and gene prediction**

632 For *M. superbum* 1065, we sequenced separately two haploid genomes, *a priori* of compatible
633 mating types based on their position in the isolated linear tetrad. We assembled these two
634 genomes separately with Canu 2.2[93] using the fastq reads files as input, and setting the -pacbio-
635 hifi parameter. For the strain collected on *D. carthusianorum*, we sequenced sporidial cultures

636 expected to correspond to mixtures of meiotic products from a diploid individual. Therefore,
637 we used the software Hifiasm 0.16.1-r375[94], which can separate haplotypes, with default
638 parameters. We performed quality assessment of the resulting assembly by computing N50 and
639 L50 statistics and by assessing genome completeness with BUSCO v5.4[95] using the
640 basidiomycota_odb10 as reference genes.
641 The two alternative mating types of M. scorzonarae were sequenced on Amherst laboratory
642 ONT platform. Longer than 1000bp of raw ONT reads were kept for genome assemblies.
643 Trimmed reads were assembled with Canu v1.7b with default parameters [93]. The resulting
644 assemblies were polished with Pilon v1.22 (https://github.com/broadinstitute/pilon/wiki) with
645 default parameters, using Illumina 150 bp paired-end reads belonging to the two mating types
646 of the same strain. To that end, short-read sequences were quality assessed using FastQC
647 (https://www.bioinformatics.babraham.ac.uk/projects/fastqc/), trimmed with Trimmomatic ()
648 using default parameters. Then 3 rounds of polishing were run iteratively with Pilon, with
649 Illumina short reads aligned to the polished assemblies obtained from the previous round and
650 indexed at each iteration using bwa-mem2 [96]. We then assessed Genome completeness with
651 BUSCO v5.4 [95] using the basidiomycota_odb10 as reference genes.

652 Repeated regions and low complexity DNA sequences were identified using RepeatModeler[97].
653 The genome was then softmasked using RepeatMasker open-4.0.9[98] with the *de novo* detected
654 repeats as well as custom libraries of candidate transposable elements (TEs) from our previous
655 studies[41] and existing fungal TEs from RepBase[99]. To minimize the rates of false negatives in
656 the gene prediction steps, we excluded from the softmasking TEs that were labeled as
657 "unknown" as their TE status was uncertain.

658 Genes were then predicted on the soft-masked genome using the software Braker version
659 2.1.6[100] which uses Diamond, ProtHint 2.6.0, GeneMark 4 and AUGUSTUS 3.4.0. To help
660 gene prediction, we combined RNAseq data from *M. superbum*, *M. intermedium* and *M.*
661 *lychnidis-dioicae*, and a set of highly conserved protein sequences previously identified across
662 multiple *Microbotryum* species. This set of proteins contains fully conserved single-copy genes
663 not overlapping with the mating-type chromosomes from 18 published *Microbotryum* genomes,
664 all predicted with the same pipeline[17,18,41,65]. The Illumina RNAseq data from 12 *M. superbum*
665 and 6 *M. intermedium* samples generated here together with 5 *M. intermedium*[39] and 17 *M.*
666 *lychnidis-dioicae*[87] samples previously obtained (Table S3) were processed with fastp[101],
667 aligned to the reference genome with the software GSNAP and GMAP[102], combined and sorted
668 with samtools[90] and filtered with Augustus[103] to keep only the unique best match (--uniq

669 option). Following Braker's documentation, we performed gene predictions separately for
670 RNAseq data and protein databases. For the gene prediction, we ran five rounds of gene
671 prediction and kept the run showing the highest BUSCO score. We eventually combined the
672 protein and RNAseq gene predictions using TSEBRA[104] and assessed the quality of the final
673 gene set with BUSCO using the basidiomycota_odb10 as reference using a dedicated workflow
674 (https://github.com/QuentinRougemont/genome_annotation). D*e novo* detection of
675 transposable elements (TEs) was performed as described previously[69].
676

677 **Orthogroup construction**

678 We performed orthology reconstruction using a set of 47 published genomes from our previous
679 work[39,41] and including the newly assembled genomes for three species studied here. The
680 *Rhodosporidium babjavae* genome was used as an outgroup[41]. We identified transposable
681 elements and predicted genes in each genome using Braker v2.1.6 with the protein database
682 built as explained above and we used in addition, for the *M. superbum*, *M. intermedium* and *M.*
683 *lychnidis-dioicae* genomes, RNAseq data from these species (n = 12, 11 and 17 conditions for
684 *M. superbum*, *M. intermedium* and *M. lychnidis-dioicae* respectively, Table S3). When
685 multiple isoforms were present, we kept the gene prediction with the longest transcript. This
686 extensive dataset was then fed to OrthoFinder[105] with default parameters to reconstruct
687 orthogroups.

688 **Identification of mating-type chromosomes**

689 We identified the contigs belonging to the mating-type chromosomes by i) detecting the contigs
690 carrying PR and HD genes using BLASTN 2.6.0[106] with the gene sequences from *M.*
691 *lagerheimii* as queries[72,107], ii) plotting the ortholog links for all contigs of our focal species
692 against the reference genome of the *M. lagerheimii* strain 1512 (a_1)[17] using Rideogram[108] iii)
693 plotting the ortholog links using Rideogram between the a_1 and a_2 genomes of our focal species.

694 We also generated circos plots using circlize[109]. In circos plots, we oriented contigs in the
695 direction involving the fewest inversions and keeping the recombining regions of the mating-
696 type chromosomes, called pseudo-autosomal regions (PARs), at the edges and non-inverted
697 between mating-type chromosomes.

698 **Analysis of selection on HD genes**

699 We aligned the coding sequences of the HD2 gene for all the *Microbotryum* species with
700 available genomes (Figure 1) using the software MACSE v2[110]. The HD2 gene that was
701 predicted as two separate genes in the a_2 genome of *M. superbum* was manually merged to
702 form one sequence, conserving the alignment with the other species. We used the RELAX
703 method from the hyphy package[111] to detect relaxed or intensified selection on the branch of
704 the HD2 gene in the a_2 genome of *M. superbum*, compared to the HD2 gene sequence in the a_1
705 and a_2 *M. lagerheimii* branches.

706 **Detection of evolutionary strata**

707 We used as a proxy of the ancestral state the chromosomal arrangement and gene order of *M.*
708 *lagerheimii,* as done in previous studies[17,65]. In *M. lagerheimii,* PR and HD loci are located on
709 different chromosomes[17]. For each species, synonymous divergence (d_S) was computed from
710 the alignment of a_1 and a_2 allele sequences, obtained with macse[112], using the yn00 v4.9f
711 program of the PAML package[113] and plotted using the ggplot2 library of R[114]. Pseudo-
712 autosomal, recombining regions were identified as regions with null synonymous divergence
713 on d_S plots, as expected in these highly selfing fungi, and with the same gene order between
714 mating types and as in *M. lagerheimii,* as assessed on circos plots. Non-recombining regions
715 were identified in contrast as regions with non-null synonymous divergence on d_S plots, and
716 being most often rearranged compared to the ancestral gene order in synteny plots. In order to
717 objectively identify the limits of evolutionary strata, we looked for changes in mean d_S along
718 the ancestral gene order along the mating-type chromosomes using a changepoint analysis
719 performed using the R package mcp[115]. This analysis relies on Bayesian regression to infer the
720 location of changes in means of the d_s values.

721 **Telomeres and centromeres**

722 To detect telomeres, we counted the occurrence of the telomere-specific motif 'TTAGGG' and
723 its reverse complement 'CCCTAA' within 1kb windows along the contigs. Peaks occur when
724 telomeres are present as they are constituted by multiple repeats of this motif. Centromeres
725 were identified by searching for the centromeric repeats previously described in *Microbotryum*
726 fungi[41,42].

727 **Trans-specific polymorphism**

728 Trans-specific polymorphism (i.e., the clustering of alleles per mating type across species) can
729 be used to study the age of recombination suppression linking genes to mating-type loci. Indeed,
730 as soon as a gene is fully linked to a mating-type locus, its alternative alleles will remain
731 associated to alternative mating types, even across speciation events. Mutations will therefore
732 accumulate independently in alleles associated with alternative mating types. In a genealogy,
733 alleles will therefore be grouped according to mating type rather than according to species. The
734 node at which the alleles associated with the alternative mating types diverge indicates the time
735 of recombination cessation[17,18,23].

736 We performed codon-based alignment with macse v2.05[110] of one-to-one orthologs of genes
737 ancestrally located on mating type chromosomes (416 genes). Gene trees were obtained with
738 IQ-TREE 1.6.1[116] with default parameters. Tree topologies were assessed using a homemade
739 awk command line, available on demand. Trees were separated into three categories: species
740 tree (a_1 and a_2 are grouped together within the species node), full trans-specific polymorphism
741 (both a_1 are grouped together and both a_2 are grouped together) and partial trans-specific
742 polymorphism (when only the a_1 or the a_2 are grouped together, or some alleles are missing).

743 A large part of the HD chromosome is collapsed in the *M. shykoffianum* genome assembly,
744 which means that it was not correctly separated between a_1 and a_2 genomes during the assembly.
745 Therefore, we could not run trans-specific polymorphism analyses in this region because the
746 genes could only be predicted in the a_1 genome assembly. However, the assembly collapse
747 means that the a_1 and a_2 alleles were highly similar, with therefore likely no trans-specific
748 polymorphism.

749 **Dating of evolutionary strata**

750 For each gene assigned to an evolutionary stratum in either of the three focal species, we
751 identified the orthologous genes in the mating-type chromosomes of four reference species
752 (eight haploid assemblies): *M. lagerheimii* and *M. intermedium*, displaying an ancestral-like
753 gene order [17], and *M. lychnidis-dioicae* and *M. silenes-dioicae*, two species for which the
754 divergence time has been estimated [74]. We filtered out orthologous groups with a copy number
755 different from one in any of the haploid genomes. For the dark ruby stratum we only
756 kept the genes assigned to the stratum in both *M. shykoffianum* and *M. superbum*. We identified
757 a minimum of 6 (dark ruby stratum) and a maximum of 31 (black stratum) orthologous groups
758 per stratum. We obtained codon-based alignments for each orthologous group with translatorX
759 [117] using muscle [118] as protein aligner. For each stratum, we concatenated the codon-based

760 alignments of its orthologous groups (alignment length range: 9528 - 75651 base-pairs) and
761 reconstructed an ultrametric tree with the least square dating method [119] under the TPM+F+G4
762 substitution model, as implemented in iqtree2 (version 2.2.6 [116]). We used the divergence time
763 between *M. lychnidis-dioicae* and *M. silenes-dioicae* as a calibration point (0.42 million
764 years[74]).

765 **Illumina sequencing and analysis**

766 A total of 165 samples were collected on several diseased *Dianthus* plants from various species
767 (*D. pavonius, D. seguieri, D. carthusianorum, D. hyssopifolius, D. albinos, D. superbus, D.*
768 *caryophyllus, D. deltoides* and *Stellaria holostea*) in several locations across Europe. For each
769 strain, diploid spores from anthers of a single flower were spread on a Petri dish containing
770 potato dextrose agar (PDA) and ampicillin, and let grow at 23°C and under artificial light.
771 Spores in a given flower are produced by a single diploid individual[120]. When placed on a
772 nutritive media, the diploid spores undergo meiosis and the resulting haploid sporidia then
773 replicate clonally. There were thousands of haploid sporidia harvested on the Petri dishes
774 representing the numerous meiotic products of a single diploid individual. However, lethal
775 alleles are sometimes found linked to one mating type in populations, so that some mixtures of
776 recovered sporidia can include only the a_1 or a_2 mating-type chromosome[58,66]. Cells were
777 harvested from the medium and stored at -20°C until DNA extraction, using the Macherey-
778 Nagel NucleoSpin Soil® kit following the manufacturer's instructions. The quality of the DNA
779 extracted was then assessed by measuring the ratio of 230/260 and 280/260 nm with a
780 NanoDrop 2000 spectrophotometer (Thermo Scientific). A Qubit 2.0 fluorometer was used to
781 measure DNA concentration. Preparation of DNA libraries for sequencing was performed
782 using the Illumina TruSeq Kits®. Paired-end libraries of 2*150 bp fragments with an insert
783 size of 300 bp were prepared with Illumina TruSeq Nano DNA Library Prep® kit. Sequencing
784 was performed on a HiSeq 2500 Illumina sequencer, with an average coverage of 10-15X. We
785 sequenced 49 genomes of *Microbotryum* strains from *D. carthusianorum*, 87 from *D. pavonius*,
786 12 from *D. seguieri*, and 17 from other hosts across western Europe. The samples were
787 collected in Italy, which is not a party of the Nagoya protocol, in the Czech Republic, Germany,
788 Finland, UK and the Netherlands, which do not regulate access to its genetic resources in
789 relation to the Nagoya Protocol, in Switzerland, where we just need to keep track of information
790 for fundamental research, and in France, where there was an exception for micro-organisms at
791 the time of sampling.

792 We followed GATK pipeline best practices for read mapping and SNP calling. Illumina reads
793 from the 165 whole genomes were mapped onto the *M. superbum* reference genome. We
794 constructed a "hybrid" reference genome by merging the whole genome MvDp−1065−A1 and
795 the two mating-type chromosomes of the MvDp−1065−A2 genome
796 (MvDp−1065−A2_tig00000068 and MvDp−1065−A2_tig00000031, respectively harboring
797 the a_2 PR and HD alleles). We mapped the reads against the hybrid reference genome using
798 BWA-MEM2[121] (https://github.com/bwa-mem2/bwa-mem2, t-4 option). For mating type-
799 chromosomes, only reads mapping to a single location were considered for further analyses.
800 We used GATK Haplotype Caller to obtain gVCF from the bam mapping files using the
801 haploid flag (ploidy =1) for the mating-type chromosomes, and using the diploid flag (ploidy
802 =2) for the rest of the genome. We used CombineGVCFs to combine gvcf of the autosomes
803 and mating-type chromosomes for a given individual, and to obtain the vcf file. We filtered out
804 highly genetically related and duplicate individuals (i.e., individuals with pairwise KING-
805 robust kinship estimates among individuals >0.354)[122] with plink version 2.0 [123], and
806 individuals with more than 20% of positions with missing genotype. We computed pairwise
807 linkage disequilibrium between genome-wide biallelic sites with minor allele frequency higher
808 than 0.25 using Plink v1.90b6.26. We used for this analysis only reads mapped to the genome
809 MvDp−1065−A1 and the 149 strains that passed filtering.

810 In our analysis of homozygosity of HD genes, we first checked the ploidy of the sequenced
811 samples at mating-type chromosomes, as they were mixtures of meiotic products with possibly
812 haplolethal alleles associated with mating types. For this goal, we performed a remapping of
813 the reads on the hybrid reference genome. Two autosomes were used as controls: tig00000012
814 and tig00000097. We calculated the median coverage along the two autosomes, as well as
815 along the PR and HD chromosomes. Strains with a median coverage lower than six reads for
816 the control autosomes were not considered further. The median coverage of the HD and PR
817 chromosomes were divided by the median coverage of the control autosome (tig00000012), to
818 get their relative coverage. Strains with a relative coverage higher than 0.7 for PR a_1 or higher
819 than 0.8 for PR a_2 were considered as haploid (23 a_1 and 14 a_2 strains). Strains with a relative
820 coverage around 0.5 (between 0.35 and 0.7) for PR a_2 also showed a coverage around 0.5 for
821 PR a_1 and were therefore considered reliable diploid (62 strains). The 17 other strains were
822 considered as having "unknown ploidy". The results were consistent when using the other
823 autosome (tig00000097) as a control. Heterozygosity of the HD chromosomes was calculated

824 for each strain on the vcf files using the command -het of vcftools, and was defined as the
825 observed number of heterozygous sites divided by the total number of sites.

826 **Tetrad isolation and PCR analyses**

827 We pulled out tetrads of *M. scorzonerae* from *Scorzonera humilis* (strain 1528, collected in
828 2018 in Cefn Cribwr, Wales, UK 51°32'08”N 3°38'52”W by Julian Woodman), *Tragopogon*
829 *pratensis* (strain 1535 collected in 2018 in Länsimäentie, Helsinki, Finland, 60°13'54.753"N
830 25°6'57.1716"E, by Juha Tuomola), *Tragopogon pratensis* (strain 1544, collected in 2018 in
831 De Weere, Netherlands, 52°44'13.33"N 4°59'22.5"E, by Justus and Maureen Houthuesen-
832 Hulshoff), and *Tragopogon porrifolius* (strain 1560 collected in 2018 in De Weere,
833 Netherlands, 52°44'13.33"N 4°59'22.5”E 2018, by Justus and Maureen Houthuesen-Hulshoff).
834 The samples were collected in Finland, the Netherlands and the UK, which do not regulate
835 access to their genetic resources in relation to the Nagoya Protocol. We also pulled out 20
836 tetrads from seven *M. superbum* strains collected on *D. pavonius* in 2019 in Garelli (Italy
837 44.1887, 7.6876). Italy is not a party of the Nagoya protocol.

838 To obtain pure haploid cultures from *M. scorzonerae* and *M. superbum* samples, teliospores
839 were first germinated by plating on water agar and incubated at room temperature for
840 approximately 12 hours. In *Microbotryum* fungi, a linear basidium containing a meiotic tetrad
841 of cells forms during germination[58]. Meiosis occurs in the basidium, yielding four haploid cells.
842 The four haploid basidium cells then undergo mitosis to form haploid sporidia. These sporidia
843 can be separated from the basidium and isolated into separate cultures by micromanipulation[58].
844 In order to assess segregation patterns of the mating-type loci across multiple meioses, sporidia
845 cells were isolated from 22 tetrads in *M. scorzonerae* and 20 tetrads in *M. superbum* samples
846 from seven *M. superbum* strains collected from *D. pavonius*. Each sporidium cell was then
847 moved by microcapillary pipetting to a potato dextrose agar (PDA) plate, and incubated at
848 room temperature. Two of every four cells in each tetrad divided only a few times after isolation
849 in *M. scorzonerae* and then stopped division. This inviability has been seen in other
850 *Microbotryum* species and is called haplo-lethality[58]. Sporidial cultures which grew
851 successfully were maintained continually on PDA and were stored as samples in silica powder
852 at -18ºC.

853 Primers were designed, using Primer3[124], that would specifically amplify, for each the PR, HD1
854 and HD2 mating-type genes, either of the two alleles that were present in the two haploid

855 reference genomes of *M. superbum*, *a priori* compatible for mating given their opposite
856 position in the tetrad[58] (Table S1).

857 For amplifying fragments of PR or HD genes, DNA templates were prepared by suspending
858 portions of fungal cultures (quantity not exceeding the tip of a sterile toothpick) in 40 µL of
859 ultrapure water. Boiling PCR was performed in a final volume of 30 µL containing 3 µL of
860 fungal suspension, 15 µL of 2X Buffer (containing a mix of dNTPs 5mM in addition of bovine
861 serum albumin (BSA) 20mg/ml, W1 detergent 1%, home made 10X Buffer (Ammonium Sulfat
862 1M, Tris HCl 1M, $MgCl_2 6H_2O$ 1M) and sterile deionized H_2O), 1.2 µL of each forward and
863 reverse primers (10 µM), 0.15 µL of Taq DNA Polymerase (5 U/µL, MP Biomedicals) and 9.8
864 µL of sterile H_2O. The touchdown PCR amplification protocol consisted of 5 min at 94°C for
865 pre-denaturation, 10 cycles of denaturation at 94°C for 30 sec, annealing at 60°C (with 1°C
866 decrements from 60°C to 50°C at every cycle) for 30 sec, and extension at 72°C for 1 min. This
867 was followed by a further 30 cycles of denaturation at 94°C for 30 sec, annealing at 50°C for
868 30 sec, and extension at 72°C for 1 min. The reaction was finished with a final extension for 5
869 min at 72°C. The PCR products were revealed and confirmed by the GelRed Nucleic Acid
870 Stain 10000X (Biotium) and photographed with UV transillumination using the VWR
871 Genosmart gel documentation system after loading on 1.5% agarose (Nippon Genetics Europe
872 GmbH)-TAE gels. PCR products were sequenced using Sanger technology at Genewiz.

873 **Mating tests and plant inoculations**

874 To check for compatibility between cultures in tetrads, mating tests were performed between
875 pairs of cultures from the same meiotic tetrad. Six-day old cultures were suspended in sterile
876 water. Suspensions were then combined in equal amounts and plated in small spots, less than
877 10µl each, onto water agar plates with 0.5ml phytol solution and onto water agar plates with
878 0.5 ml sterile water. The phytol solution was 0.006% phytol and 0.8% ethanol[58]. Phytol has
879 been shown to induce hyphal growth in *Microbotryum* fungi[125]. Plates were refrigerated at 5ºC.
880 Spots were checked for hyphae using an inverted scope between 2 and 4 days after plating. We
881 used cultures of *M. superbum* sporidia of opposite PR mating types but identical HD alleles to
882 inoculate seeds of *Dianthus chinesis* as previously described[58]. We grew the plants in the
883 greenhouse and checked for symptoms in anthers. The species *D. chinesis* was used as it is
884 easier to grow under the greenhouse and make it flower than *D. pavonius* or *D. carthusianorum*
885 and the focal *Microbotryum* fungi are found on various Dianthus hosts in nature.

886 **Softwares for figures**

887 For figures illustrating synteny, we used the package circlize[126] or Rideogram[108] based on
888 alignments performed with mummer[127]. We used ggplot2 for plotting d_S values. For RNAseq
889 mapping illustration, we used the package karyoploteR[92].

890

891 **Data availability**

892 RNASeq data for all experiments listed in this section are available in GEO at NCBI, Accession
893 Numbers/Record GSE233508 for the *M. superbum* data.

894

895 **Acknowledgements**

896 This work was supported by the Louis D. Foundation award and EvolSexChrom ERC advanced
897 grant #832352 to T. G, a National Institute of Health (NIH) grant R15GM119092 to M. E. H.,
898 and a National Science Foundation (NSF) grant #2007449 to M.H.P. We thank Klara
899 Koupilova, Janis Antonovics, Emme Bruns and Juha Tuomola for the *M. v. Dianthus* strains,
900 Justus & Maureen Houthuesen-Hulshoff, Julian Woodman, Juha Tuomola for the *M.*
901 *scorzonerae* strains, and Emme Bruns for *Dianthus* plants. We thank Julian Woodman for the
902 picture of *M. scorzonareae*.

903

904 **Author contributions**

905 T.G., M.E.H., A.C. and R.R.d.l.V. conceptualized the study, acquired funding and supervised
906 the study. M.E.H., T.G. and A.C. acquired the *Microbotryum* strains. A.S. extracted DNA for
907 PacBio sequencing. M.E.H. and W.J.M. sequenced and analysed the *M. scorzonerae* genome.
908 E.L., P.J., Q.R., L.B. and R.R.d.l.V. analyzed the PacBio genomes. A.C. acquired the Illumina
909 genomes and performed SNP calling. P.J. and E.L. analysed the Illumina genomes. M.E.H. and
910 J.G. performed tetrad isolation and mating tests. A.L., E.C., M.E.H. and J.G. performed tetrad
911 segregation analyses. M.H.P. and R.K.H. acquired the expression data. R.R.d.l.V. analyzed the
912 RNAseq data. E.L., P.J. and R.R.d.l.V. produced the figures. T.G. and E.L. wrote the
913 manuscript draft with contributions by P.J., M.E.H., Q.R., M.H.P. and R.K.H. All authors
914 edited the manuscript. The final version of the manuscript was prepared by E.L., R.R.d.l.V.
915 and T.G.

916

917

918

919

920 **REFERENCES**

921

922 1 Lande, R. & Schemske, D. The evolution of self-fertilization and inbreeding depression
923 in plants. I. Genetic models. *Evolution* **39**, 24-40 (1985).
924 2 Charlesworth, D. & Charlesworth, B. Inbreeding depression and its evolutionary
925 consequences. *Annu Rev Ecol Evol Syst* **18**, 237-268 (1987).
926 3 Charlesworth, D., Morgan, M. & Charlesworth, B. Inbreeding depression, genetic load,
927 and the evolution of outcrossing rates in a multilocus system with no linkage. *Evolution* **44**,
928 1469-1489 (1990).
929 4 Charlesworth, D. Plant sex determination and sex chromosomes. *Heredity* **88**, 94-101
930 (2002).
931 5 Igic, B., Lande, R. & Kohn, J. Loss of self-incompatibility and its evolutionary
932 consequences. *Int J Plant Sci* **169**, 93-104 (2008).
933 6 Hereford, J. Does selfing or outcrossing promote local adaptation? . *Am J Bot* **97**, 298-
934 302 (2010).
935 7 Lande, R. Evolution of phenotypic plasticity in colonizing species. *Mol Ecol* **24**, 2038-
936 2045 (2015).
937 8 Nieuwenhuis, B. P. S. *et al.* Evolution of uni- and bifactorial sexual compatibility
938 systems in fungi. *Heredity* **111**, 445-455, doi:10.1038/hdy.2013.67 (2013).
939 9 Goldberg, E. & Igić, B. Tempo and mode in plant breeding system evolution. *Evolution*
940 **66**, 3701-3709 (2012).
941 10 Chantha, S., Herman, A., Platts, A., Vekemans, X. & Schoen, D. Secondary evolution
942 of a self-incompatibility locus in the Brassicaceae genus *Leavenworthia*. *PLoS Biol* **11**,
943 e1001560 (2013).
944 11 Hanschen, E., Herron, M., Wiens, J., Nozaki, H. & Michod, R. Repeated evolution and
945 reversibility of self-fertilization in the volvocine green algae. *Evolution* **72**, 386-398 (2018).
946 12 Beukeboom, L. & Perrin, N. 92-93 (Oxford University Press, Oxford, 2014).
947 13 Vekemans, X., Poux, C., Goubet, P. & Castric, V. The evolution of selfing from
948 outcrossing ancestors in Brassicaceae: What have we learned from variation at the S-locus? .
949 *J Evol Biol* **27**, 1372-1385 (2014).
950 14 Billiard, S. *et al.* Having sex, yes, but with whom? Inferences from fungi on the
951 evolution of anisogamy and mating types. *Biol Rev* **86**, 421-442 (2011).
952 15 Billiard, S., López-Villavicencio, M., Hood, M. & Giraud, T. Sex, outcrossing and mating
953 types: unsolved questions in fungi and beyond. *J Evol Biol* **25**, 1020-1038 (2012).
954 16 Coelho, M. A., Bakkeren, G., Sun, S., Hood, M. E. & Giraud, T. Fungal Sex: The
955 Basidiomycota. *Microbiology Spectrum* **5**, 1-30, doi:10.1128/microbiolspec.FUNK-0046-2016
956 (2017).
957 17 Branco, S. *et al.* Evolutionary strata on young mating-type chromosomes despite the
958 lack of sexual antagonism. *Proceedings of the National Academy of Sciences* **114**, 7067-7072,
959 doi:10.1073/pnas.1701658114 (2017).
960 18 Branco, S. *et al.* Multiple convergent supergene evolution events in mating-type
961 chromosomes. *Nature Communications* **9**, 2000, doi:10.1038/s41467-018-04380-9 (2018).
962 19 Charlesworth, D. The status of supergenes in the 21st century: recombination
963 suppression in Batesian mimicry and sex chromosomes and other complex adaptations.
964 *Evolutionary Applications* **9**, 74-90, doi:10.1111/eva.12291 (2016).
965 20 Charlesworth, D. Evolution of recombination rates between sex chromosomes.
966 *Philosophical Transactions of the Royal Society B-Biological Sciences* **372**,
967 doi:10.1098/rstb.2016.0456 (2017).
968 21 Charlesworth, D. When and how do sex-linked regions become sex chromosomes?
969 *Evolution* **75**, 569-581, doi:10.1111/evo.14196 (2021).
970 22 Bergero, R. & Charlesworth, D. The evolution of restricted recombination in sex
971 chromosomes. *Trends in Ecology & Evolution* **24**, 94-102, doi:10.1016/j.tree.2008.09.010
972 (2009).

23 Hartmann, F. E. *et al.* Recombination suppression and evolutionary strata around mating-type loci in fungi: documenting patterns and understanding evolutionary and mechanistic causes. *New Phytologist* **229**, 2470-2491, doi:10.1111/nph.17039 (2021).
24 Vittorelli, N. *et al.* Stepwise recombination suppression around the mating-type locus in the fungus *Schizothecium tetrasporum* (Ascomycota, Sordariales). *PLoS Genetics* **19**, e1010347 (2022).
25 Ironside, J. E. No amicable divorce? Challenging the notion that sexual antagonism drives sex chromosome evolution. *Bioessays* **32**, 718-726, doi:10.1002/bies.200900124 (2010).
26 Charlesworth, D., Charlesworth, B. & Marais, G. Steps in the evolution of heteromorphic sex chromosomes. *Heredity* **95** 118-128 (2005).
27 Wright, A. E., Dean, R., Zimmer, F. & Mank, J. E. How to make a sex chromosome. *Nature Communications* **7**, 12087, doi:10.1038/ncomms12087 (2016).
28 Bazzicalupo, A. L., Carpentier, F., Otto, S. P. & Giraud, T. Little evidence of antagonistic selection in the evolutionary strata of fungal mating-type chromosomes *(Microbotryum lychnidis-dioicae)*. *G3-Genes Genomes Genetics* **9**, 1987-1998, doi:10.1534/g3.119.400242 (2019).
29 Jeffries, D. L., Gerchen, J. F., Scharmann, M. & Pannell, J. R. A neutral model for the loss of recombination on sex chromosomes. *Philosophical Transactions of the Royal Society B-Biological Sciences* **376**, doi:10.1098/rstb.2020.0096 (2021).
30 Kent, T. V., Uzunovic, J. & Wright, S. I. Coevolution between transposable elements and recombination. *Philosophical Transactions of the Royal Society B-Biological Sciences* **372**, doi:10.1098/rstb.2016.0458 (2017).
31 Jay, P., Tezenas, E., Véber, A. & Giraud, T. Sheltering of deleterious mutations explains the stepwise extension of recombination suppression on sex chromosomes and other supergenes. *PLoS Biology* **20**, e3001698, doi:10.1371/journal.pbio.3001698 (2022).
32 Lenormand, T. & Roze, D. Y recombination arrest and degeneration in the absence of sexual dimorphism. *Science* **375**, 663-+, doi:10.1126/science.abj1813 (2022).
33 Jay, P., Jeffries, D., Hartmann, F. E., Véber, A. & Giraud, T. Why do sex chromosomes progressively lose recombination? . *Trends in Genetics* **in press** (2024).
34 Hill, W. G. & Robertson, A. The effect of linkage on limits to artificial selection. *Genetics Research* **8**, 269-294, doi:10.1017/S001667230800949X (1966).
35 Muller, H. J. Some genetic aspects of sex. *The American Naturalist* **66**, 118-138 (1932).
36 Charlesworth, B. & Charlesworth, D. The degeneration of Y chromosomes. *Philosophical Transactions of the Royal Society B-Biological Sciences* **355**, 1563-1572, doi:10.1098/rstb.2000.0717 (2000).
37 Charlesworth, D. The timing of genetic degeneration of sex chromosomes. *Phil. Trans. R. Soc. B* **376**, 20200093 (2021).
38 Bachtrog, D. Y-chromosome evolution : emerging insights into processes of Y-chromosome degeneration. *Nature Reviews Genetics* **14**, 113-124, doi:10.1038/nrg3366 (2013).
39 Carpentier, F. *et al.* Tempo of degeneration across independently evolved nonrecombining regions. *Molecular Biology and Evolution* **39**, doi:10.1093/molbev/msac060 (2022).
40 Fontanillas, E. *et al.* Degeneration of the nonrecombining regions in the mating-type chromosomes of the anther-smut fungi. *Molecular Biology and Evolution* **32**, 928-943, doi:10.1093/molbev/msu396 (2015).
41 Duhamel, M. *et al.* Onset and stepwise extensions of recombination suppression are common in mating-type chromosomes of *Microbotryum* anther-smut fungi. *Journal of Evolutionary Biology* **35**, 1619-1634, doi:10.1111/jeb.13991 (2022).
42 Badouin, H. *et al.* Chaos of rearrangements in the mating-type chromosomes of the anther-smut fungus *Microbotryum lychnidis-dioicae*. *Genetics* **200**, 1275-1284, doi:10.1534/genetics.115.177709 (2015).

43 Kües, U., James, T. Y. & Heitman, J. in *Evolution of Fungi and Fungal-Like Organisms* (eds S. Pöggeler & J. Wöstemeyer) Pp. 97–160 (Springer, 2011).
44 Bakkeren, G. & Kronstad, J. W. Linkage of mating-type loci distinguishes bipolar from tetrapolar mating in basidiomycetous smut fungi. *Proceedings of the National Academy of Sciences of the United States of America* **91**, 7085-7089, doi:10.1073/pnas.91.15.7085 (1994).
45 Xu, J. *et al.* Dandruff-associated *Malassezia* genomes reveal convergent and divergent virulence traits shared with plant and human fungal pathogens. *Proceedings of the National Academy of Sciences of the United States of America* **104**, 18730-18735, doi:10.1073/pnas.0706756104 (2007).
46 Coelho, M. A., Ianiri, G., David-Palmaa, M. & Heitman, J. Frequent transitions in mating-type locus chromosomal organization in Malassezia and early steps in sexual reproduction. *PNAS* **120**, e2305094120 (2023).
47 James, T. Y., Srivilai, P., Kues, U. & Vilgalys, R. Evolution of the bipolar mating system of the mushroom *Coprinellus disseminatus* from its tetrapolar ancestors involves loss of mating-type-specific pheromone receptor function. *Genetics* **172**, 1877-1891, doi:10.1534/genetics.105.051128 (2006).
48 Chen, B. Z. *et al.* Fruiting body formation in *Volvariella volvacea* can occur independently of its MAT-a-controlled bipolar mating system, enabling homothallic and heterothallic life cycles. *G3-Genes Genomes Genetics* **6**, 2135-2146, doi:10.1534/g3.116.030700 (2016).
49 Kues, U. *et al.* A chimeric homeodomain protein causes self-incompatibility and constitutive sexual development in the mushroom *Coprinus cinereus*. *Embo Journal* **13**, 4054-4059, doi:10.1002/j.1460-2075.1994.tb06722.x (1994).
50 Hood, M. E. *et al.* Distribution of the anther-smut pathogen non species of the Caryophyllaceae. *New Phytologist* **187**, 217-229, doi:10.1111/j.1469-8137.2010.03268.x (2010).
51 Hartmann, F. E. *et al.* in *Annual Review of Phytopathology, Vol 57, 2019* Vol. 57 *Annual Review of Phytopathology* (eds J. E. Leach & S. E. Lindow) 431-457 (2019).
52 Le Gac, M., Hood, M. E., Fournier, E. & Giraud, T. Phylogenetic evidence of host-specific cryptic species in the anther smut fungus. *Evolution* **61**, 15-26, doi:10.1111/j.1558-5646.2007.00002.x (2007).
53 Refrégier, G. *et al.* Cophylogeny of the anther smut fungi and their caryophyllaceous hosts: Prevalence of host shifts and importance of delimiting parasite species for inferring cospeciation. *BMC Evolutionary Biology* **8**, doi:10.1186/1471-2148-8-100 (2008).
54 Hood, M. E., Antonovics, J. & Koskella, B. Shared forces of sex chromosome evolution in haploids and diploids. *Genetics* **168**, 141-146 (2004).
55 Feurtey, A. *et al.* Strong phylogeographic co-structure between the anther-smut fungus and its white campion host. *New Phytologist* **212**, 668-679, doi:https://doi.org/10.1111/nph.14125 (2016).
56 Giraud, T., Yockteng, R., Lopez-Villavicencio, M., Refregier, G. & Hood, M. E. The mating system of the anther smut fungus, *Microbotryum violaceum*: selfing under heterothallism. *Euk. Cell* **7**, 765-775 (2008).
57 Hartmann, F. E. *et al.* Congruent population genetic structures and divergence histories in anther-smut fungi and their host plants Silene italica and the Silene nutans species complex. *Molecular Ecology* **29**, 1154-1172, doi:https://doi.org/10.1111/mec.15387 (2020).
58 Hood, M. E. & Antonovics, J. Intratetrad mating, heterozygosity, and the maintenance of deleterious alleles in *Microbotryum violaceum (= Ustilago violacea)*. *Heredity* **85**, 231-241, doi:10.1046/j.1365-2540.2000.00748.x (2000).
59 Alexander, H. M., Thrall, P. H., Antonovics, J., Jarosz, A. M. & Oudemans, P. V. Population dynamics and genetics of plant disease: a case study of anther-smut disease. *Ecology* **77**, 990-996 (1996).
60 Antonovics, J., Iwasa, Y. & Hassel, M. P. A generalized model of parasitoid, veneral, and vector-based transmission processes. *Am. Nat.* **145**, 661-675 (1995).

1079 61 Hood, M. E., Antonovics, J. & Heishman, H. Karyotypic similarity identifies multiple
1080 host-shifts of a pathogenic fungus in natural populations. *Infection, Genetics and Evolution* **2**,
1081 167-172 (2003).
1082 62 Hartmann, F. E. *et al.* Higher gene flow in sex-related chromosomes than in autosomes
1083 during fungal divergence. *Molecular Biology and Evolution* **37**, 668-682,
1084 doi:10.1093/molbev/msz252 (2020).
1085 63 Zakharov, I. A. [Intratetrad mating and its genetic and evolutionary consequences].
1086 *Genetika* **41**, 508-519 (2005).
1087 64 Zakharov, I. A. Intratetrad mating as the driving force behind the formation of sex
1088 chromosomes in fungi. *Trends in Genetics and Evolution* **6**, doi:
1089 10.24294/tge.v24296i24291.24252 (2023).
1090 65 Carpentier, F. *et al.* Convergent recombination cessation between mating-type genes
1091 and centromeres in selfing anther-smut fungi. *Genome Research* **29**, 944-953,
1092 doi:10.1101/gr.242578.118.5 (2019).
1093 66 Thomas, A., Shykoff, J., Jonot, O. & Giraud, T. Sex-ratio bias in populations of the
1094 phytopathogenic fungus Microbotryum violaceum from several host species. *International*
1095 *Journal of Plant Sciences* **164**, 641-647, doi:10.1086/375374 (2003).
1096 67 Kaltz, O. & Shykoff, J. A. Sporidial mating-type ratios of teliospores from natural
1097 populations of the anther smut fungus *Microbotryum* (equals *Ustilago) violaceum*. *International*
1098 *Journal of Plant Sciences* **158**, 575-584, doi:10.1086/297470 (1997).
1099 68 Oudemans, P. V. *et al.* The distribution of mating-type bias in natural populations of
1100 the anther-smut Ustilago violacea on Silene alba in Virginia. *Mycologia* **90**, 372-381,
1101 doi:10.2307/3761395 (1998).
1102 69 Duhamel, M., Hood, M. E., Rodriguez de la Vega, R. C. & Giraud, T. Dynamics of
1103 transposable element accumulation in the non-recombining regions of mating-type
1104 chromosomes in anther-smut fungi. *Nature Communications* **14**, 5692 (2023).
1105 70 Horns, F., Petit, E. & Hood, M. E. Massive expansion of *Gypsy*-Like retrotransposons
1106 in *Microbotryum* fungi. *Genome Biology and Evolution* **9**, 363-371, doi:10.1093/gbe/evx011
1107 (2017).
1108 71 Hood, M. E. & Antonovics, J. Mating Within the Meiotic Tetrad and the Maintenance of
1109 Genomic. **1759**, 1751-1759 (2004).
1110 72 Devier, B., Aguileta, G., Hood, M. & Giraud, T. Ancient trans-specific polymorphism at
1111 pheromone receptor genes in basidiomycetes. *Genetics* **181**, 209–223 (2009).
1112 73 Day, A. & Jones, J. The production and characteristics of diploids in *Ustilago violacea*.
1113 *Genet. Res., Camb.* **11**, 63-81 (1968).
1114 74 Gladieux, P. *et al.* Maintenance of fungal pathogen species that are specialized to
1115 different hosts: allopatric divergence and introgression through secondary contact. *Molecular*
1116 *Biology and Evolution* **28**, 459-471, doi:10.1093/molbev/msq235 (2011).
1117 75 Lee, N., Bakkeren, G., Wong, K., Sherwood, J. E. & Kronstad, J. W. The mating-type
1118 and pathogenicity locus of the fungus Ustilago hordei spans a 500-kb region. *Proceedings of*
1119 *the National Academy of Sciences of the United States of America* **96**, 15026-15031,
1120 doi:10.1073/pnas.96.26.15026 (1999).
1121 76 Fraser, J. A. *et al.* Convergent evolution of chromosomal sex-determining regions in
1122 the animal and fungal kingdoms. *Plos Biol.* **2**, 2243-2255 (2004).
1123 77 Rabe, F. *et al.* A complete toolset for the study of *Ustilago bromivora* and
1124 *Brachypodium sp* as a fungal-temperate grass pathosystem. *Elife* **5**, doi:10.7554/eLife.20522
1125 (2016).
1126 78 Sun, S., Coelho, M. A., Heitman, J. & Nowrousian, M. Convergent evolution of linked
1127 mating-type loci in basidiomycete fungi. *PLoS Genet.* **15**, e1008365 (2019).
1128 79 Yi, R. *et al.* Genomic structure of the A mating-type locus in a bipolar basidiomycete,
1129 Pholiota nameko. *Mycol Res.* **113**, 240-248 (2009).
1130 80 Wang, Y.-W. *et al.* Invasive Californian death caps develop mushrooms unisexually
1131 and bisexually. *Nature Communications* **14**, 6560 (2023).

1132 81 Cabrita, A. *et al.* Multiple pathways to homothallism in closely related yeast lineages
1133 in the Basidiomycota. *mBio* **12**, 10.1128/mbio.03130-03120, doi:10.1128/mbio.03130-20
1134 (2021).
1135 82 de Vienne, D. M., Hood, M. E. & Giraud, T. Phylogenetic determinants of potential host
1136 shifts in fungal pathogens. *Journal of Evolutionary Biology* **22**, 2532-2541, doi:10.1111/j.1420-
1137 9101.2009.01878.x (2009).
1138 83 Petit, E. *et al.* Co-occurrence and hybridization of anther-smut pathogens specialized
1139 on Dianthus hosts. *Molecular Ecology* **26**, 1877-1890, doi:https://doi.org/10.1111/mec.14073
1140 (2017).
1141 84 Denchev, C. M., Giraud, T. & Hood, M. E. Three new species of anthericolous smut
1142 fungi on Caryophyllaceae. *Mycologica Balcanica* **6**, 79-84 (2009).
1143 85 Liu, T., Tian, H., He, S. & Guo, L. *Microbotryum scorzonerae* (Microbotryaceae), new
1144 to China, on a new host plant. *Mycotaxon* **108**, 245-247 (2009).
1145 86 Le Gac, M., Hood, M. E. & Giraud, T. Evolution of reproductive isolation within a
1146 parasitic fungal species complex. *Evolution* **61**, 1781-1787, doi:10.1111/j.1558-
1147 5646.2007.00144.x (2007).
1148 87 Perlin, M. H. *et al.* Sex and parasites: Genomic and transcriptomic analysis of
1149 *Microbotryum lychnidis-dioicae,* the biotrophic and plant-castrating anther smut fungus. *BMC*
1150 *genomics* **16**, 1-24, doi:10.1186/s12864-015-1660-8 (2015).
1151 88 San Toh, S. *et al.* Pas de deux: an Intricate dance of anther smut and its host. **8**, 505-
1152 518, doi:10.1534/g3.117.300318 (2018).
1153 89 Li, H. Minimap2: pairwise alignment for nucleotide sequences. *Bioinformatics* **34**,
1154 3094-3100, doi:10.1093/bioinformatics/bty191 (2018).
1155 90 Danecek, P. *et al.* Twelve years of SAMtools and BCFtools. *GigaScience* **10**, giab008,
1156 doi:10.1093/gigascience/giab008 (2021).
1157 91 Diesh, C. *et al.* JBrowse 2: a modular genome browser with views of synteny and
1158 structural variation. *Genome Biology* **24**, 74, doi:10.1186/s13059-023-02914-z (2023).
1159 92 Gel, B. & Serra, E. karyoploteR: an R/Bioconductor package to plot customizable
1160 genomes displaying arbitrary data. *Bioinformatics* **33**, 3088-3090,
1161 doi:10.1093/bioinformatics/btx346 (2017).
1162 93 Koren, S. *et al.* Canu: scalable and accurate long-read assembly via adaptive k-mer
1163 weighting and repeat separation. *Genome Research* **27**, 722-736 (2017).
1164 94 Cheng, H., Concepcion, G. T., Feng, X., Zhang, H. & Li, H. Haplotype-resolved *de*
1165 *novo* assembly using phased assembly graphs with hifiasm. *Nat Methods* **18**, 170-175 (2021).
1166 95 Manni, M., Berkeley, M. R., Seppey, M., Simão, F. A. & Zdobnov, E. M. BUSCO Update:
1167 Novel and Streamlined Workflows along with Broader and Deeper Phylogenetic Coverage for
1168 Scoring of Eukaryotic, Prokaryotic, and Viral Genomes. *Molecular Biology and Evolution* **38**,
1169 4647-4654, doi:10.1093/molbev/msab199 (2021).
1170 96 Walker, B. J. *et al.* Pilon: An Integrated Tool for Comprehensive Microbial Variant
1171 Detection and Genome Assembly Improvement. *PLOS ONE* **9**, e112963,
1172 doi:10.1371/journal.pone.0112963 (2014).
1173 97 Flynn, J. M. *et al.* RepeatModeler2 for automated genomic discovery of transposable
1174 element families. **117**, 9451-9457, doi:10.1073/pnas.1921046117 (2020).
1175 98 Smit, A., Hubley, R. & Green, P. RepeatMasker Open-4.0.
1176 <http://www.repeatmasker.org> (2013-2015).
1177 99 Bao, W., Kojima, K. K. & Kohany, O. Repbase Update, a database of repetitive
1178 elements in eukaryotic genomes. *Mobile DNA* **6**, 11, doi:10.1186/s13100-015-0041-9 (2015).
1179 100 Bruna, T., Hoff, K. J., Lomsadze, A., Stanke, M. & Borodovsky, M. BRAKER2:
1180 automatic eukaryotic genome annotation with GeneMark-EP+ and AUGUSTUS supported by
1181 a protein database. *NAR Genomics and Bioinformatics* **3**, lqaa108 (2021).
1182 101 Chen, S., Zhou, Y., Chen, Y. & Gu, J. fastp: an ultra-fast all-in-one FASTQ
1183 preprocessor. *Bioinformatics* **34**, i884-i890, doi:10.1093/bioinformatics/bty560 (2018).
1184 102 Wu, T. D., Reeder, J., Lawrence, M., Becker, G. & Brauer, M. J. in *Statistical Genomics:*
1185 *Methods and Protocols* (eds Ewy Mathé & Sean Davis) 283-334 (Springer New York, 2016).

103 Keller, O., Kollmar, M., Stanke, M. & Waack, S. A novel hybrid gene prediction method employing protein multiple sequence alignments. *Bioinformatics* **27**, 757-763, doi:10.1093/bioinformatics/btr010 (2011).
104 Gabriel, L., Hoff, K. J., Brůna, T., Borodovsky, M. & Stanke, M. TSEBRA: transcript selector for BRAKER. **22**, 566, doi:10.1186/s12859-021-04482-0 (2021).
105 Emms, D. M. & Kelly, S. OrthoFinder: phylogenetic orthology inference for comparative genomics. *Genome Biology* **20**, 238, doi:10.1186/s13059-019-1832-y (2019).
106 Altschul, S. F., Gish, W., Miller, W., Myers, E. W. & Lipman, D. J. Basic local alignment search tool. *Journal of Molecular Biology* **215**, 403-410, doi:https://doi.org/10.1016/S0022-2836(05)80360-2 (1990).
107 Petit, E. *et al.* Linkage to the mating-type locus across the genus *Microbotryum*: insights into non-recombining chromosomes. *Evolution* **66**, 3519-3533 (2012).
108 Hao, Z. *et al.* RIdeogram: drawing SVG graphics to visualize and map genome-wide data on the idiograms. *PeerJ. Computer science* **6**, e251, doi:10.7717/peerj-cs.251 (2020).
109 Gu, Z., Gu, L., Eils, R., Schlesner, M. & Brors, B. circlize Implements and enhances circular visualization in R. *Bioinformatics* **30**, 2811-2812, doi:10.1093/bioinformatics/btu393 (2014).
110 Ranwez, V., Douzery, E. J. P., Cambon, C., Chantret, N. & Delsuc, F. MACSE v2: Toolkit for the alignment of coding sequences accounting for frameshifts and stop codons. *Molecular Biology and Evolution* **35**, 2582-2584, doi:10.1093/molbev/msy159 (2018).
111 Wertheim, J. O., Murrell, B., Smith, M. D., Kosakovsky Pond, S. L. & Scheffler, K. RELAX: Detecting Relaxed Selection in a Phylogenetic Framework. *Molecular Biology and Evolution* **32**, 820-832, doi:10.1093/molbev/msu400 (2015).
112 Ranwez, V., Harispe, S., Delsuc, F. & Douzery, E. J. P. MACSE: Multiple alignment of coding sequences accounting for frameshifts and stop codons. *PLOS ONE* **6**, e22594, doi:10.1371/journal.pone.0022594 (2011).
113 Yang, Z. PAML 4: Phylogenetic analysis by maximum likelihood. *Molecular Biology and Evolution* **24**, 1586-1591, doi:10.1093/molbev/msm088 (2007).
114 Wickham, H. *Ggplot2: Elegant Graphics for Data Analysis (2nd. ed.)*. (Springer Publishing Company, 2009).
115 Lindeløv, J. K. Mcp: An R package for regression with multiple change points. *https://doi.org/10.31219/osf.io/fzqxv* (2020).
116 Minh, B. Q. *et al.* IQ-TREE 2: New models and efficient methods for phylogenetic inference in the genomic era. *Molecular Biology and Evolution* **37**, 1530-1534, doi:10.1093/molbev/msaa015 (2020).
117 Abascal, F., Zardoya, R. & Telford, M. J. TranslatorX: multiple alignment of nucleotide sequences guided by amino acid translations. *Nucleic acids research* **38**, W7-13, doi:10.1093/nar/gkq291 (2010).
118 Edgar, R. C. MUSCLE: Multiple sequence alignment with high accuracy and high throughput. *Nucleic acids research* **32**, 1792-1797, doi:10.1093/nar/gkh340 (2004).
119 To, T.-H., Jung, M., Lycett, S. & Gascuel, O. Fast dating using least-squares criteria and algorithms. *Systematic biology* **65**, 82-97, doi:10.1093/sysbio/syv068 (2016).
120 Lopez-Villavicencio, M. *et al.* Multiple infections by the anther smut pathogen are frequent and involve related strains. *PloS Pathogens* **3**, e176 (2007).
121 Vasimuddin, M., Misra, S., Li, H. & Aluru, S. Efficient architecture-aware acceleration of BWA-MEM for multicore systems. *2019 IEEE International Parallel and Distributed Processing Symposium (IPDPS)*, 314-324 (2019).
122 Manichaikul, A. *et al.* Robust relationship inference in genome-wide association studies. *Bioinformatics* **26**, 2867-2873, doi:10.1093/bioinformatics/btq559 (2010).
123 Chang, C. C. *et al.* Second-generation PLINK: rising to the challenge of larger and richer datasets. *Gigascience* **4**, 7, doi:10.1186/s13742-015-0047-8 (2015).
124 Untergasser, A. *et al.* Primer3--new capabilities and interfaces. *Nucleic Acids Res.* **40**, e115 (2012).

125 Castle, A. J. & Day, A. W. Isolation and Identification of α -Tocopherol as an Inducer of the Parasitic Phase of *Ustilago violacea Phytopathology* **74**, 1194-1200 (1984).

126 Gu, Z., Gu, L., Eils, R., Schlesner, M. & Brors, B. circlize implements and enhances circular visualization in R. *Bioinformatics* **30**, 2811-2812, doi:10.1093/bioinformatics/btu393 (2014).

127 Kurtz, S. *et al.* Versatile and open software for comparing large genomes. *Genome Biology* **5**, R12, doi:10.1186/gb-2004-5-2-r12 (2004).

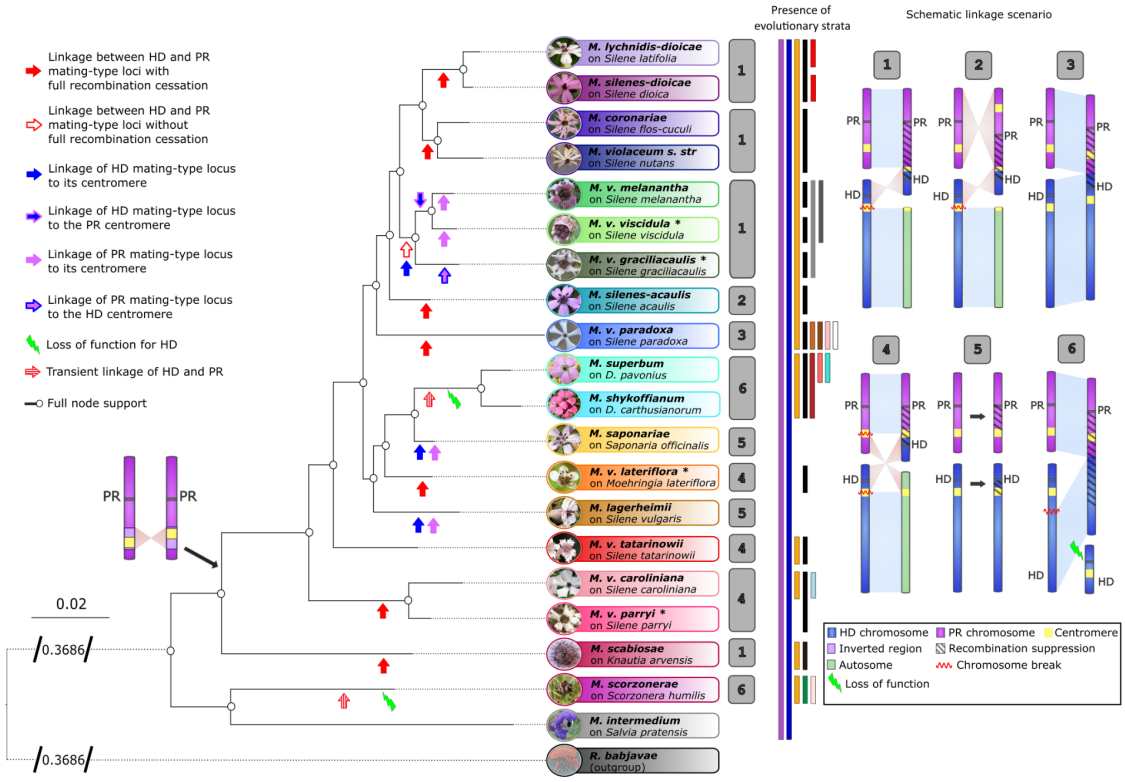

Figure 1: Species tree with pictures of diseased plants parasitized by the different *Microbotryum* species and showing chromosomal arrangements of the mating-type chromosomes compared to the ancestral state. Arrows of different colors on the tree branches indicate mating-type locus linkage, or their linkage to centromeres, or loss of function. Colored bars at the right of the phylogeny indicate the presence of evolutionary strata suppression recombination beyond mating-type loci. Pictures are from Michael E. Hood and Julian Woodman.

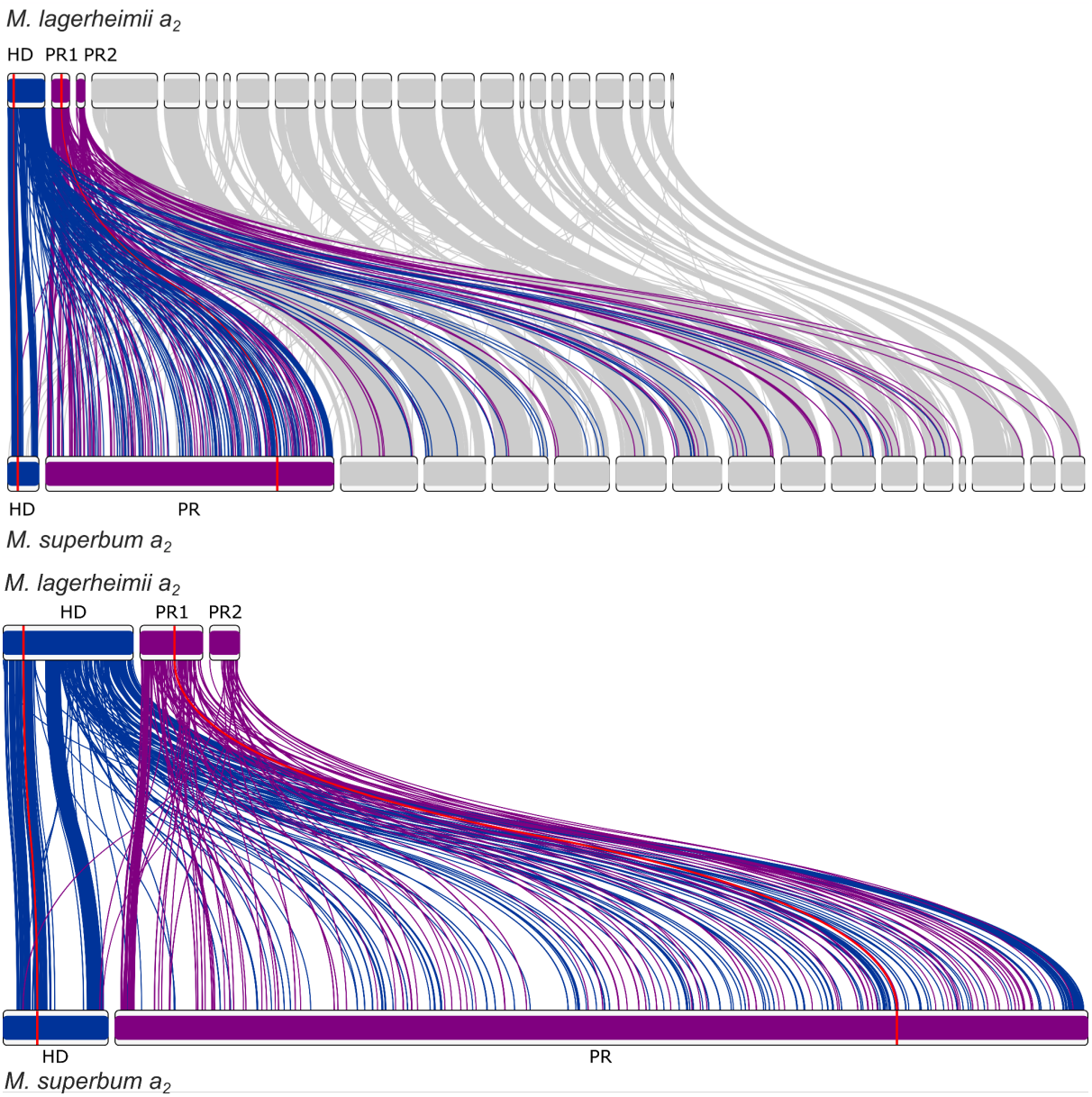

Figure 2: Synteny and rearrangements between the a_1 genomes of *Microbotryum superbum* and *M. lagerheimii*, with all contigs (top) or only the mating-type chromosomes (bottom). The *M. lagerheimii* genome represents a proxy for the ancestral state before recombination suppression and with two separate mating-type chromosomes. The HD mating-type chromosome from *M. lagerheimii* is represented in blue and the PR mating-type chromosome in purple (splitted into two scaffolds), with links to orthologous genes to the *M. superbum* mating-type chromosomes. The positions of the HD and PR mating-type genes are indicated in red and by red links between the two genomes. The PR chromosome shows a substantial increase in size and a chaos of rearrangements.

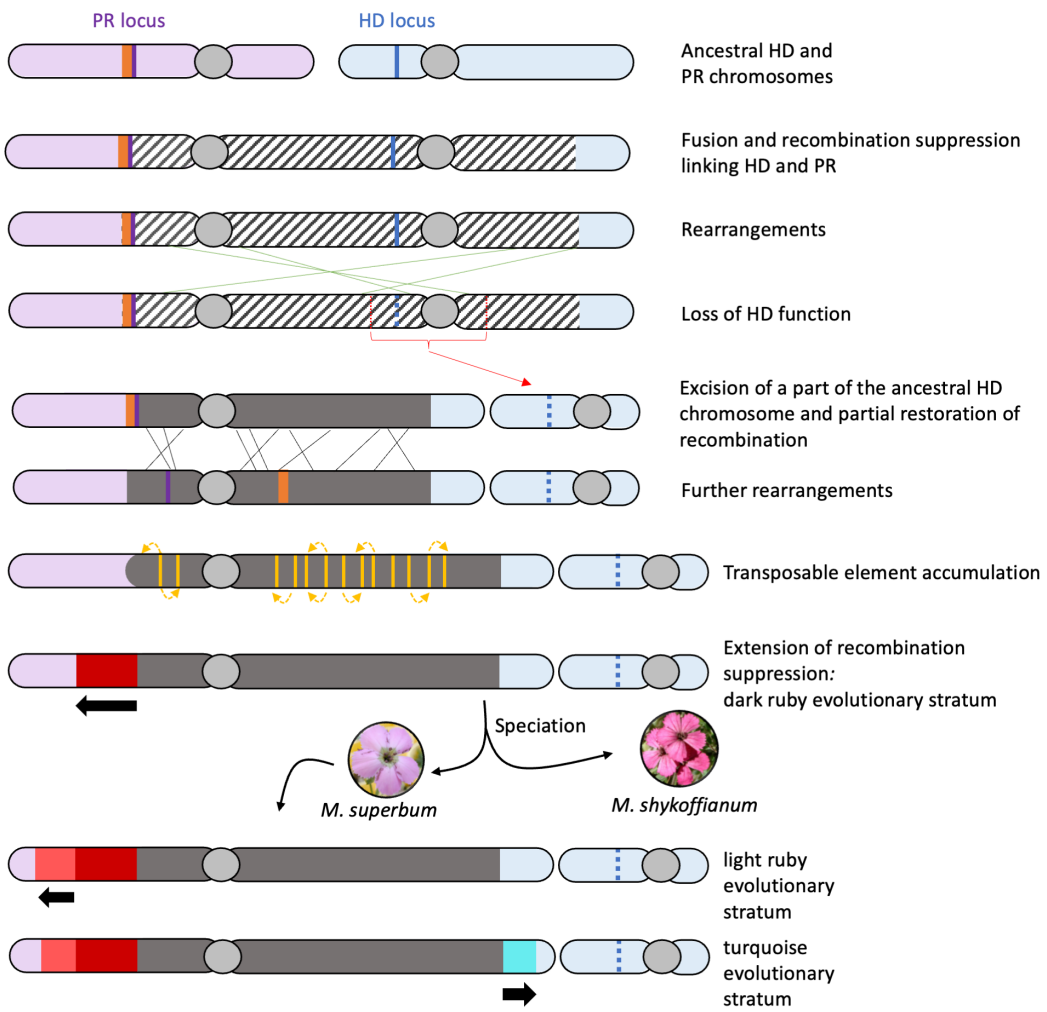

Figure 3: Inferred scenario for the evolution of the mating-type chromosomes in *Microbotryum superbum* and *M. shykoffianum*. Pictures of the diseased plants parasitized by the two species are shown. Recombination suppression is figured by colors corresponding to the different evolutionary strata.

1281

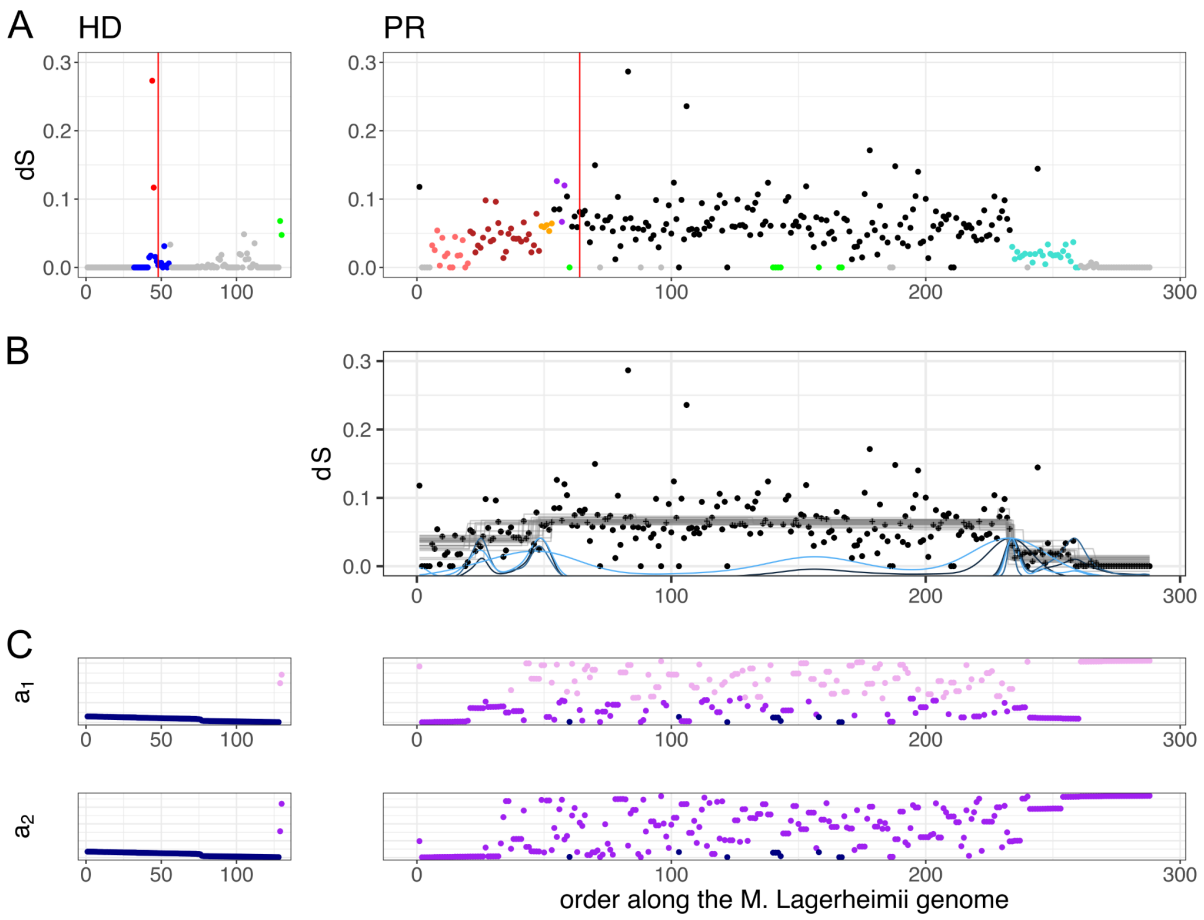

1282 **Figure 4: Differentiation and rearrangements between the mating-type chromosomes in**
1283 ***Microbotryum superbum*. A)** Per-gene synonymous divergence (d_S) plotted along the ancestral
1284 gene order (taking as proxy the gene order along the *M. lagerheimii* mating-type chromosomes),
1285 the HD chromosome at left and the PR chromosome at right; the points are colored according
1286 to their evolutionary stratum assignment: turquoise, light and dark ruby for the *M. superbum*
1287 specific evolutionary strata, black for the evolutionary stratum shared by *M. superbum* and *M.*
1288 *shykoffianum,* blue, orange and purple for the ancient evolutionary strata shared by most
1289 *Microbotryum* species. The pseudo-autosomal regions (PARs) are in grey. The green points
1290 correspond to genes that were ancestrally on the PR chromosome but found in the HD
1291 chromosomes in *M. superbum* or reciprocally. **B)** Change-point analysis identifying changes in
1292 mean dS levels. **C)** Rearrangements compared to the ancestral gene order figured by plotting
1293 the gene rank in the current gene order (b1 in the a_1 genome and b_2 in the a_2 genome) as a
1294 function of the gene rank in the ancestral gene order.

1295

1296

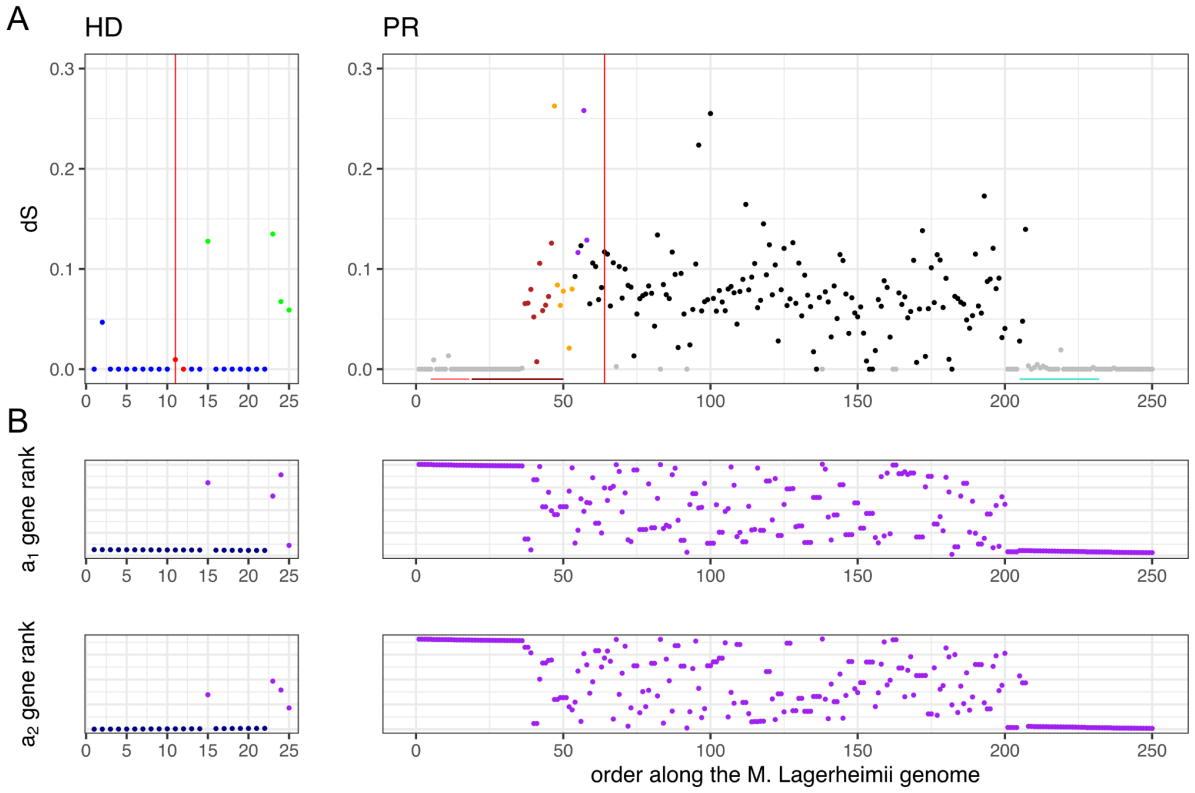

Figure 5: Differentiation and rearrangements between the mating-type chromosomes in *Microbotryum shykoffianum*. a) Per-gene synonymous divergence (d_S) plotted along the ancestral gene order (taking as proxy the gene order along the *M. lagerheimii* mating-type chromosomes)**,** the HD chromosome at left and the PR chromosome at right. The points are colored according to their evolutionary stratum assignment: turquoise, light ruby and half of the dark ruby region for the *M. superbum* specific evolutionary strata, black and the other half of the dark ruby for the evolutionary stratum shared by *M. superbum* and *M. shykoffianum,* blue, orange and purple for the ancient evolutionary strata shared by most *Microbotryum* species. The pseudo-autosomal regions (PARs) are in grey. The position of the *M. superbum* specific evolutionary strata are indicated by color bars at the bottom. The green points correspond to genes that were ancestrally on the PR chromosome but found in the HD chromosomes in *M. superbum* or reciprocally. **B)** Rearrangements compared to the ancestral gene order figured by plotting the gene rank in the current gene order (b_1 in the a_1 genome and b_2 in the a_2 genome) as a function of the gene rank in the ancestral gene order.

1313

1314

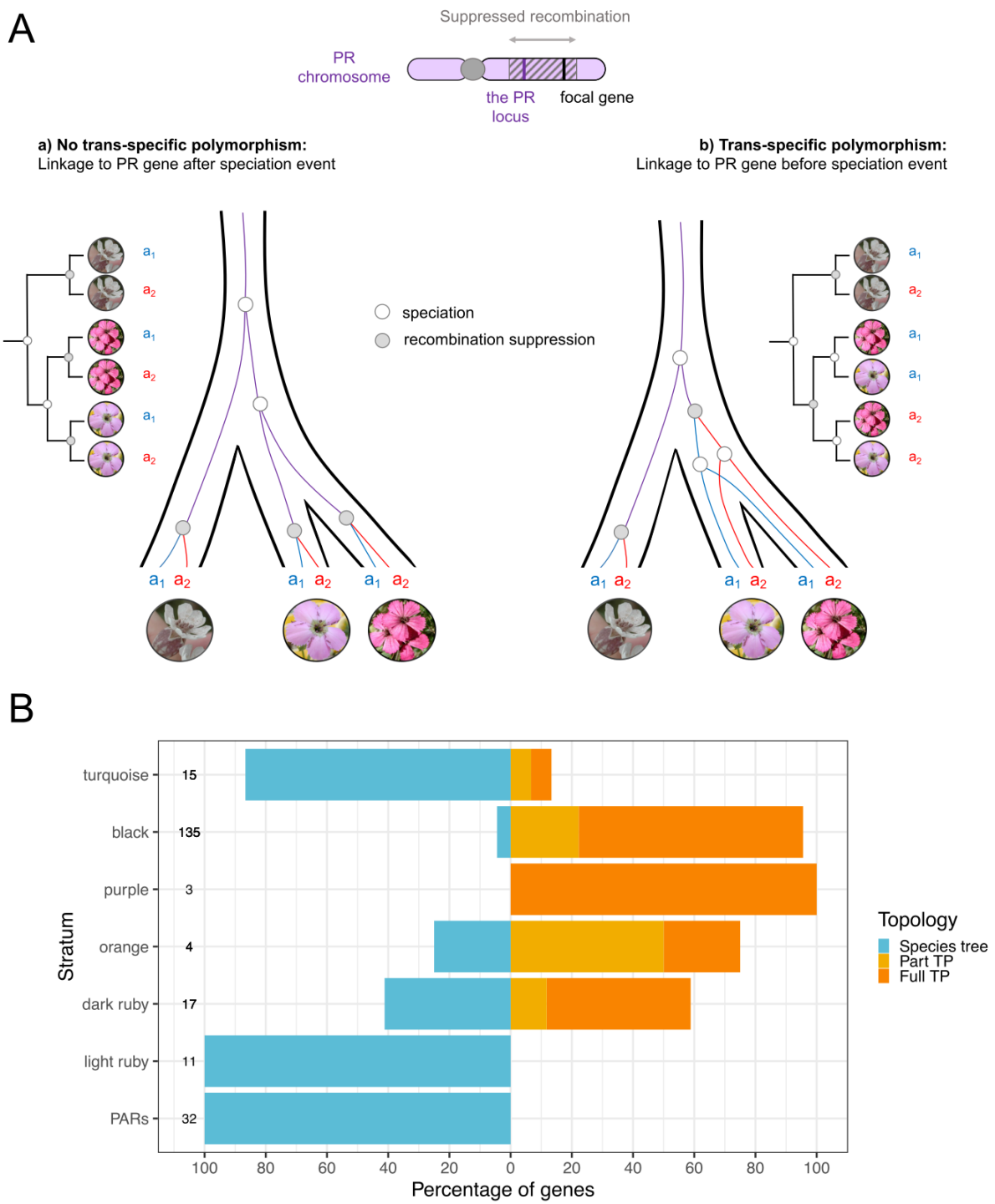

1315 **Figure 6: Trans-specific polymorphism (TP) of genes present along the mating-type chromosomes**
1316 **in *Microbotryum superbum*, considering also *M. shykoffianum* and *M. lagerheimii.* A)** Schematic
1317 representation of trans-specific polymorphism in genes completely linked to mating-type loci by
1318 suppressed recombination, allowing to assess whether recombination cessation occurred before or after
1319 speciation, here between *M. lagerheimii, M. superbum* and *M. shykoffianum*. **B)** Percentage of genes
1320 within each evolutionary stratum with the following genealogy pattern: full trans-specific

1321 polymorphism (i.e., across both *M. superbum* and *M. shykoffianum*), partial trans-specific
1322 polymorphism (i.e., with only one allele showing clustering by mating type and the other by species, or
1323 with one allele missing, i.e. not informative), and no trans-specific polymorphism or unresolved. The
1324 total number of genes analyzed per stratum is indicated at the left of each barplot. The PARs (pseudo-
1325 autosomal regions) correspond to the PR chromosome PARs pooled together.

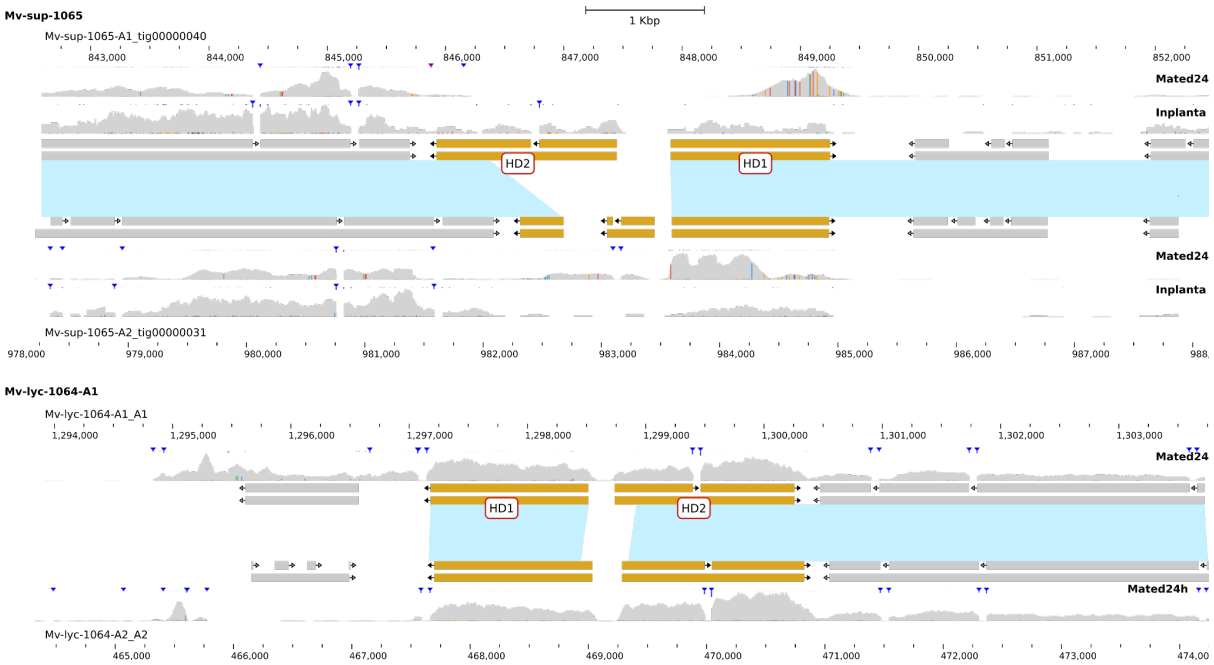

Figure 7: Structure and expression of the HD genes in *Microbotryum superbum* (A) and *M. lychnidis-dioicae* (B). In the middle of each panel, the coding sequences of the genes present in the a_1 HD chromosome and the a_2 HD chromosome are represented by rectangles (upper rectangles correspond to the coding sequence features and lower rectangles to the transcript features), and the direction of the transcription is indicated by an arrow. The HD2 and HD1 genes are represented in yellow boxes. The blue areas represent the syntenic regions between the a_1 and a_2 sequences. Above and below the rectangles, the level of expression is represented and annotated according to the condition of the RNAseq extraction (mated 24h or *in planta*).

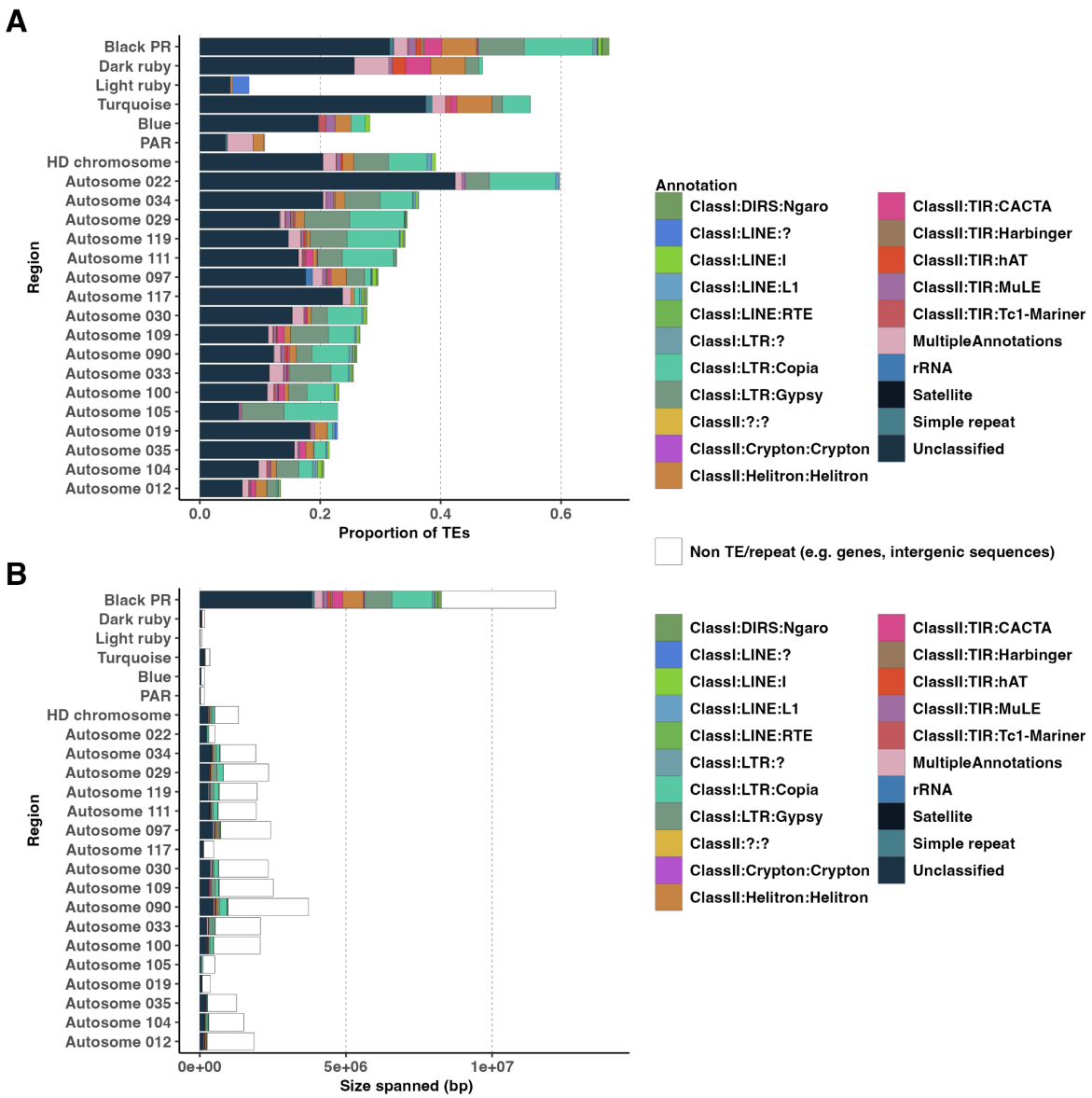

Figure 8: Scaffold size and transposable element (TE) content in the genome of *Microbotryum superbum* a$_1$, as a proportion (A) or absolute content in base pair (bp, B). The relative proportions of transposable element classes in each scaffold is represented by the sizes of the colored bars. The PR chromosome is separated into its different evolutionary strata (blue, black, turquoise, light and dark ruby) and the pseudo-autosomal regions (PAR). The blue stratum on the HD chromosome is also separated from the rest of the chromosome. Only scaffolds longer than 300kb are displayed.

1351 **SUPPLEMENTARY FIGURES**

1352

1353

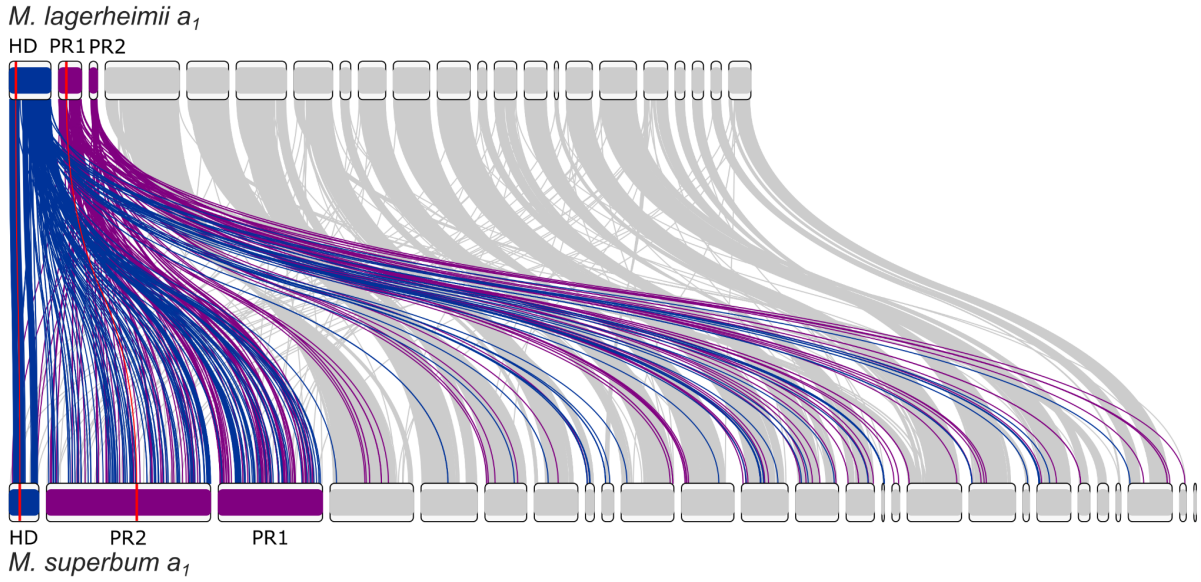

1354

1355

1356

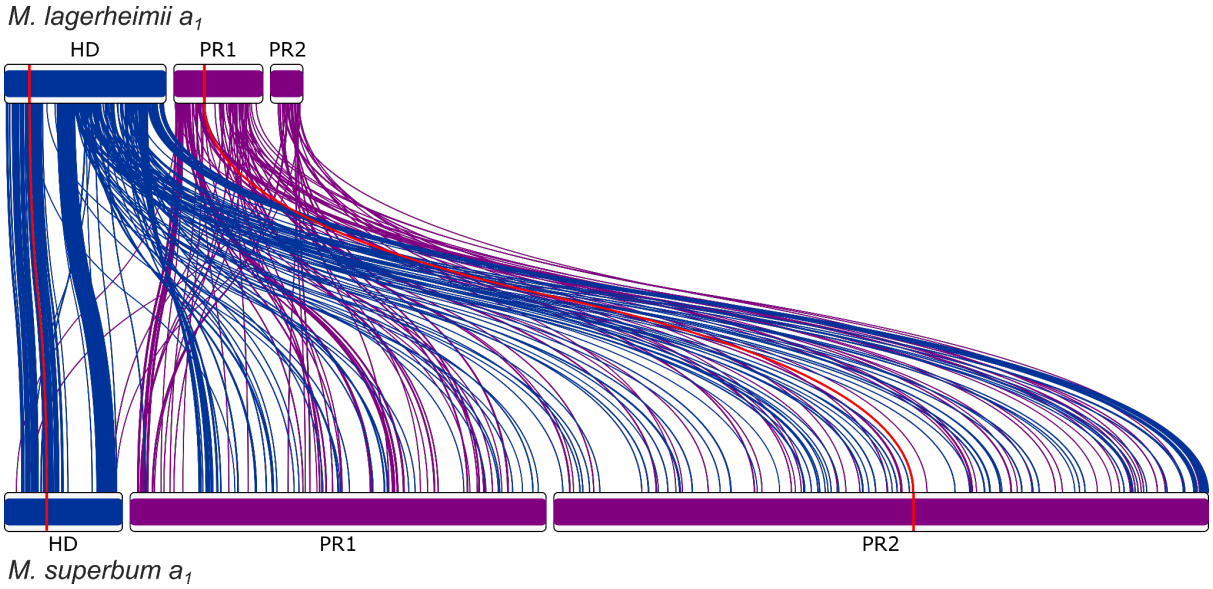

1357 **Figure S1: Synteny and rearrangements between the a_1 genomes of *Microbotryum***
1358 ***superbum* and *M. lagerheimii*, with all contigs (top) or only the mating-type chromosomes**
1359 **(bottom).** The *M. lagerheimii* genome represents a proxy for the ancestral state before
1360 recombination suppression and with two separate mating-type chromosomes. The HD mating-
1361 type chromosome from *M. lagerheimii* is represented in blue and the PR mating-type
1362 chromosome in purple (splitted into two scaffolds), with links to orthologous genes to the *M.*
1363 *superbum* mating-type chromosomes. The positions of the HD and PR mating-type genes are

1364 indicated in red and by red links between the two genomes. The PR chromosome shows a
1365 substantial increase in size and a chaos of rearrangements.

1366

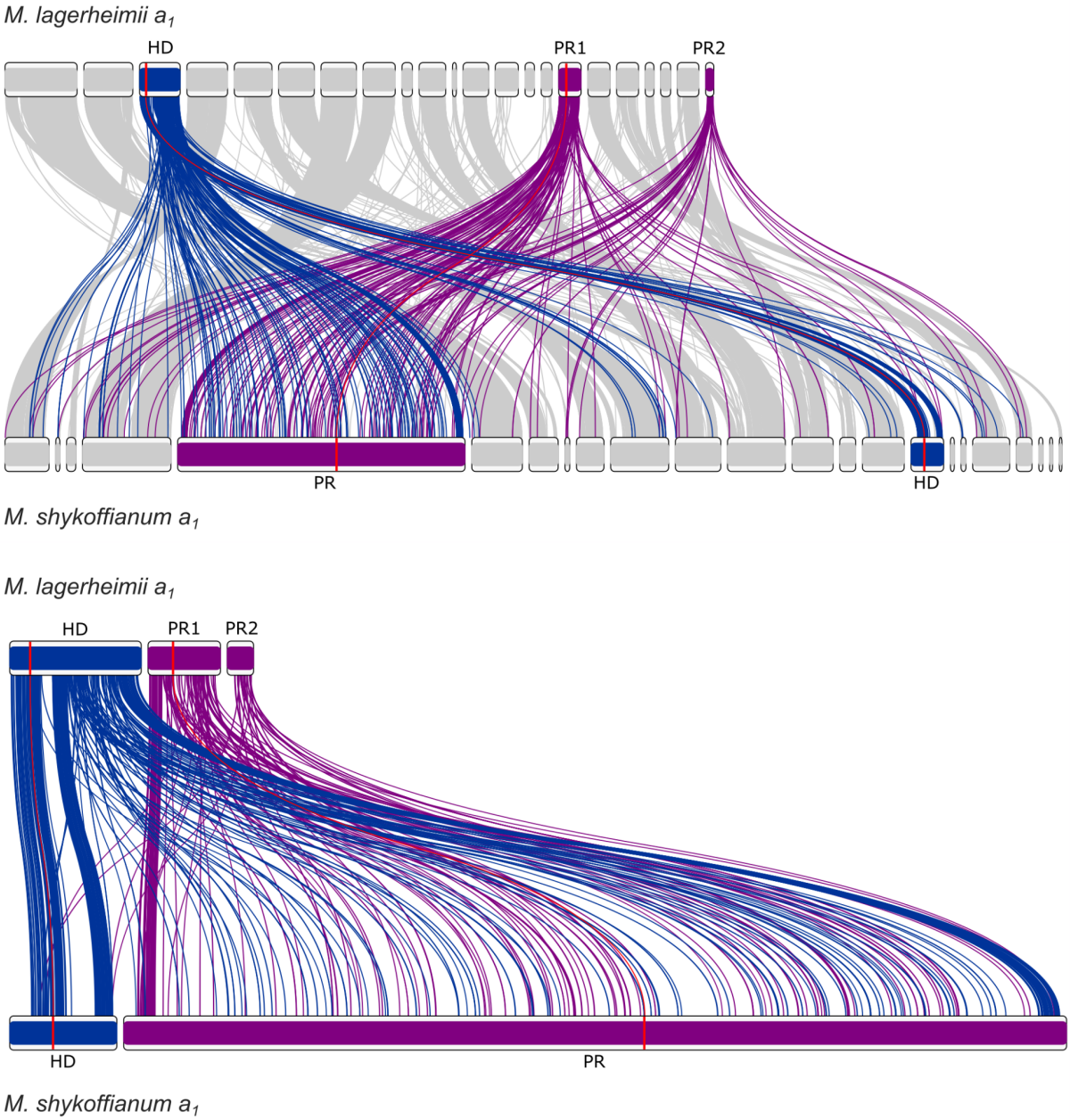

1367 **Figure S2: Synteny and rearrangements between the a_1 genomes of *Microbotryum***
1368 ***shykoffianum* and *M. lagerheimii*, with all contigs (top) or only the mating-type**
1369 **chromosomes (bottom).** The *M. lagerheimii* genome represents a proxy for the ancestral state
1370 before recombination suppression and with two separate mating-type chromosomes. The HD
1371 mating-type chromosome from *M. lagerheimii* is represented in blue and the PR mating-type
1372 chromosome in purple (splitted into two scaffolds), with links to orthologous genes to the *M.*
1373 *superbum* mating-type chromosomes. The positions of the HD and PR mating-type genes are
1374 indicated in red and by red links between the two genomes. The PR chromosome shows a
1375 substantial increase in size and a chaos of rearrangements.

1376
1377

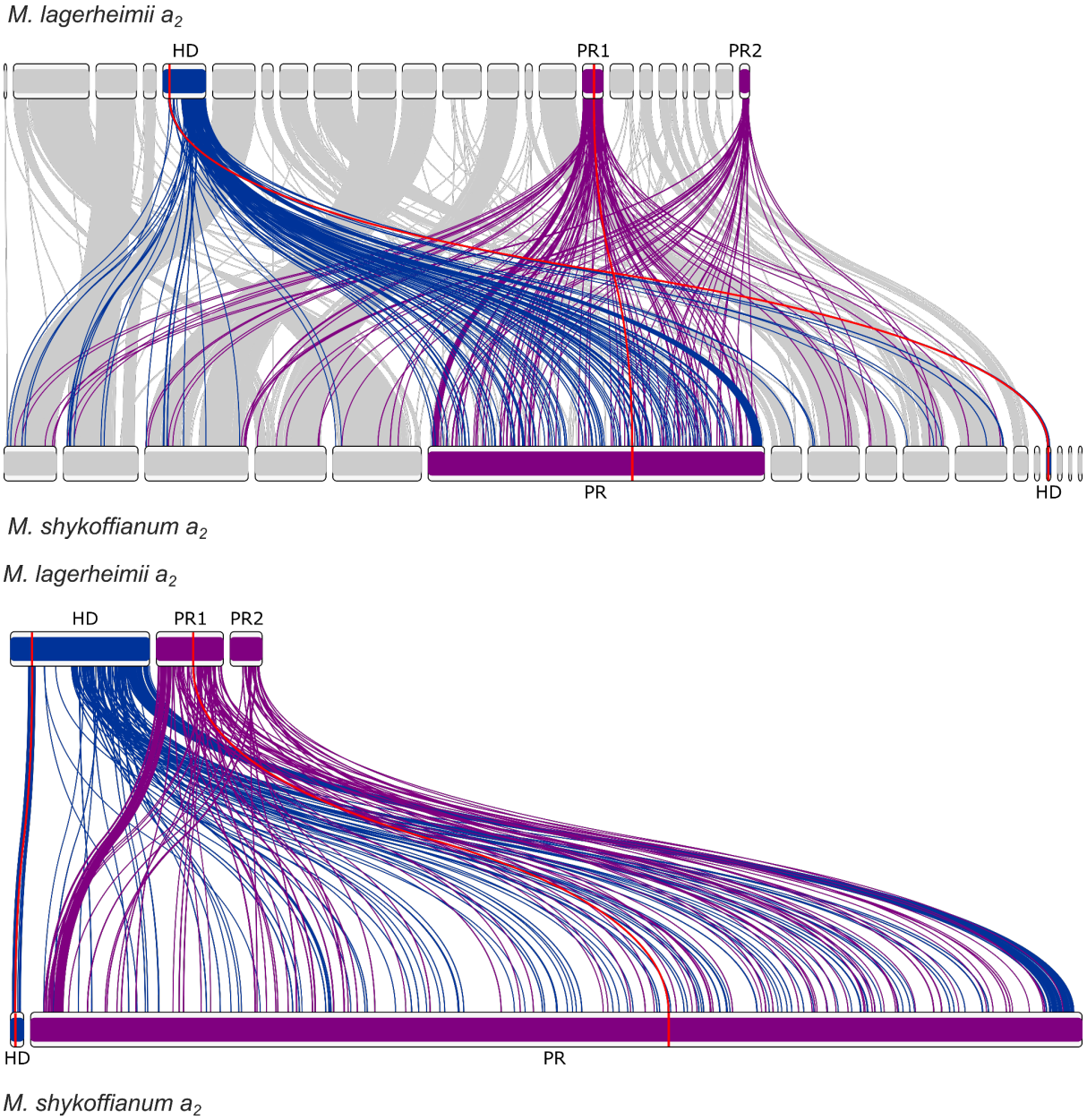

1378

1379 **Figure S3: Synteny and rearrangements between the a2 genomes of *Microbotryum***
1380 ***shykoffianum* and *M. lagerheimii*, with all contigs (top) and only the mating-type**
1381 **chromosomes (bottom).** The *M. lagerheimii* genome represents a proxy for the ancestral state
1382 before recombination suppression and with two separate mating-type chromosomes. The HD
1383 mating-type chromosome from *M. lagerheimii* is represented in blue and the PR mating-type
1384 chromosome in purple (splitted into two scaffolds), with links to orthologous genes to the *M.*
1385 *superbum* mating-type chromosomes. The positions of the HD and PR mating-type genes are
1386 indicated in red and by red links between the two genomes. The PR chromosome shows a
1387 substantial increase in size and a chaos of rearrangements.

1388

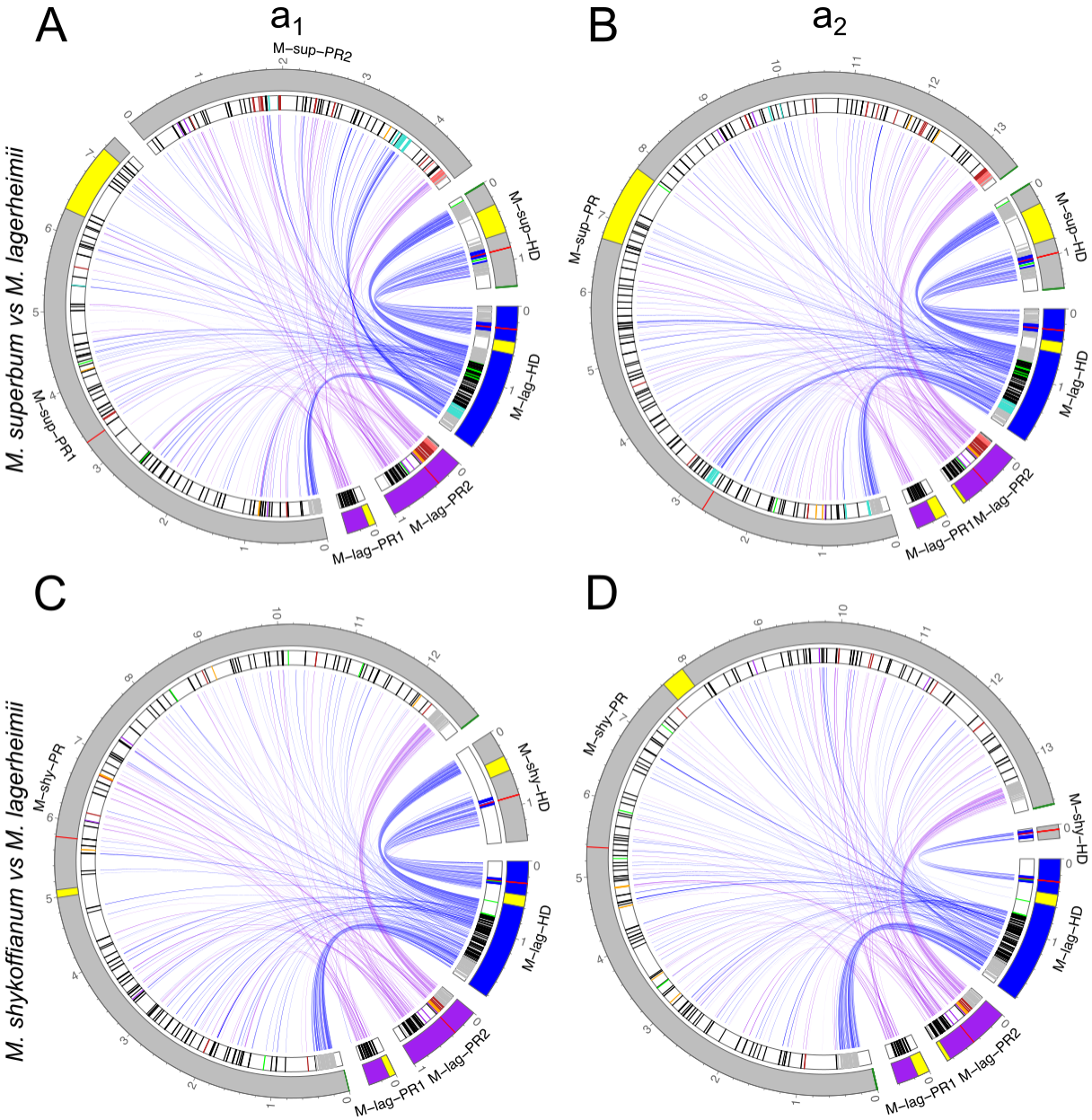

Figure S4: Synteny and rearrangements between the a_1 (left) and a_2 (right) HD and PR mating-type chromosomes of *Microbotryum superbum* (A-B) and *Microbotryum shykoffianum* (C-D) compared to those of *M. lagerheimii*. Links are represented between orthologous genes, in blue for the genes on the *M. lagerheimii* HD mating-type chromosome and in purple for the *M. lagerheimii* PR mating-type chromosome. The HD and PR mating-type genes are indicated in red. Centromeres are figured in yellow and telomeres in dark green on the outer track. The strata are indicated by their color on the inner track. Genes that have moved from the ancestral short HD chromosome arm to current PR chromosome, or reciprocally, are in green on the inner track.

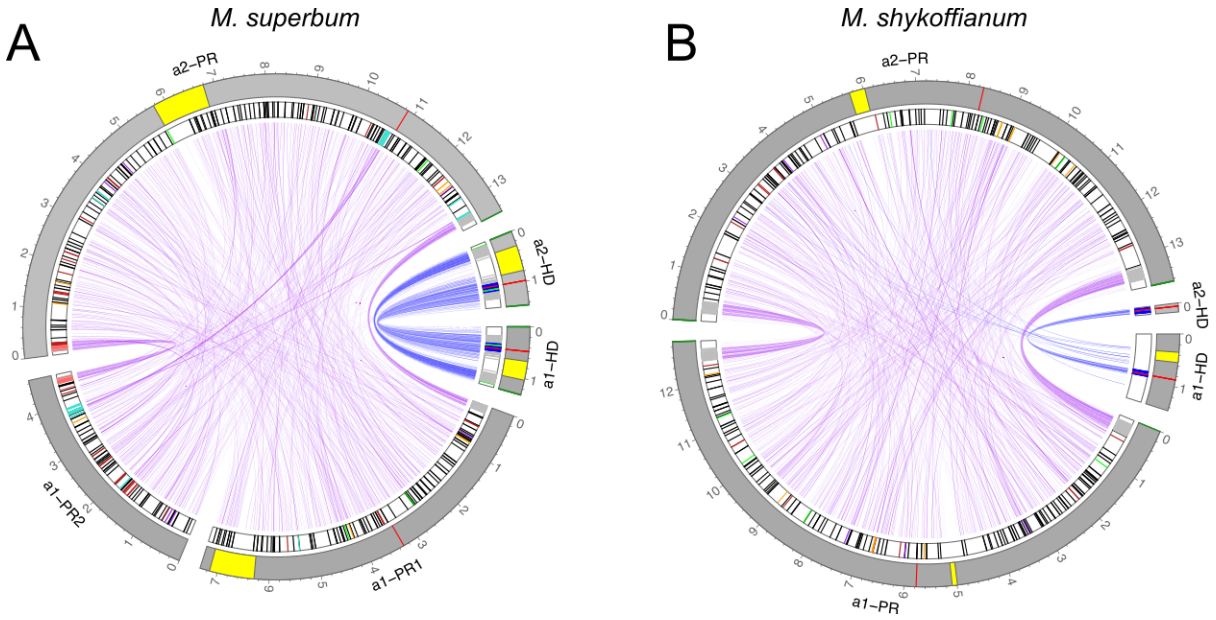

Figure S5: Synteny and rearrangements between the a_1 and a_2 mating-type chromosomes (HD and PR chromosomes) of *Microbotryum superbum* (A) and *Microbotryum shykoffianum* (B). Links are represented between orthologous genes, colors corresponding to the evolutionary strata. The HD and PR mating-type genes are indicated in red. Centromeres are figured in yellow and telomeres in dark green on the outer track. The strata are indicated by their color on the inner track. Genes that have moved from ancestral short HD chromosome arm to current PR chromosome, or reciprocally, are in green on the inner track.

1408

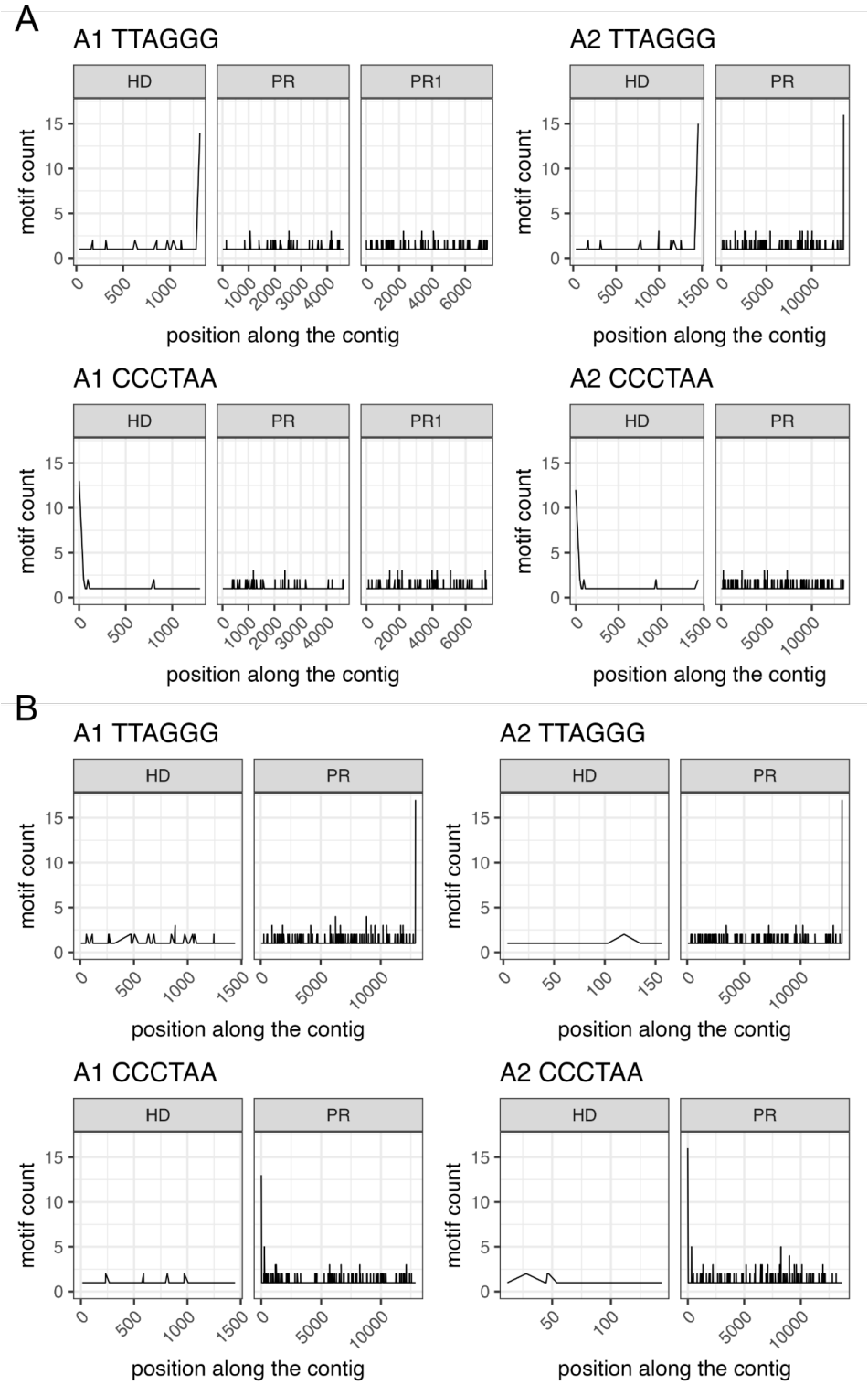

1409 **Figure S6: Telomere motifs count over 1kb windows for *Microbotryum violaceum superbum* (A)**
1410 **and *M. shykoffianum* (B).** Top panel corresponds to the motif TTAGGG for a_1 and a_2 contigs, and
1411 bottom panel to the inverse complement CCCTAA for a_1 and a_2 contigs.

1412

1413

1414
1415
1416

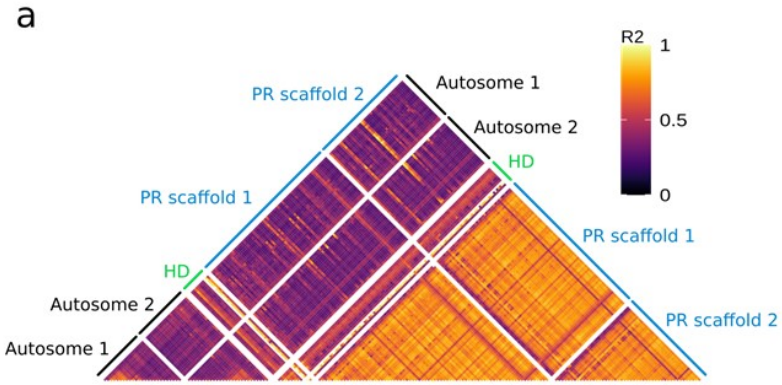

1417 b

1418

1419

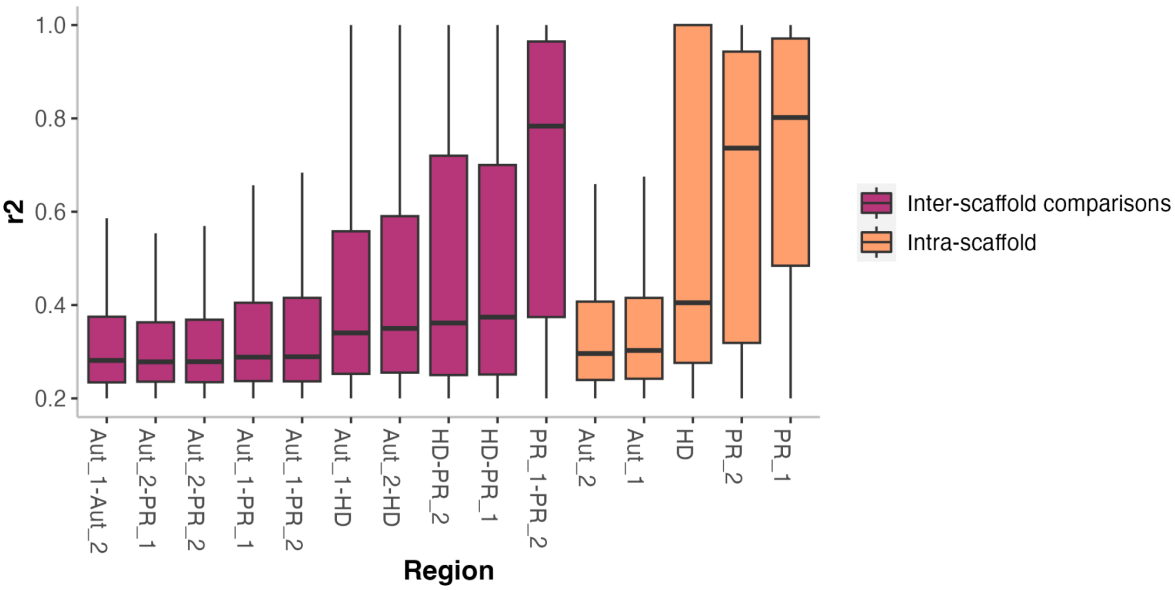

1420 **Figure S7: Linkage disequilibrium between the mating-type chromosomes and two autosomes in**
1421 **the a_1 genome of *Microbotryum superbum.*** Linkage disequilibrium as measured by r^2 is represented
1422 with colors along chromosomes (a) and summarized with boxplots (b). The two autosomes are called
1423 Aut1 and Aut2, and the two contigs of the PR chromosomes in the a_1 genome are called PR1 and PR2.

1424

1425

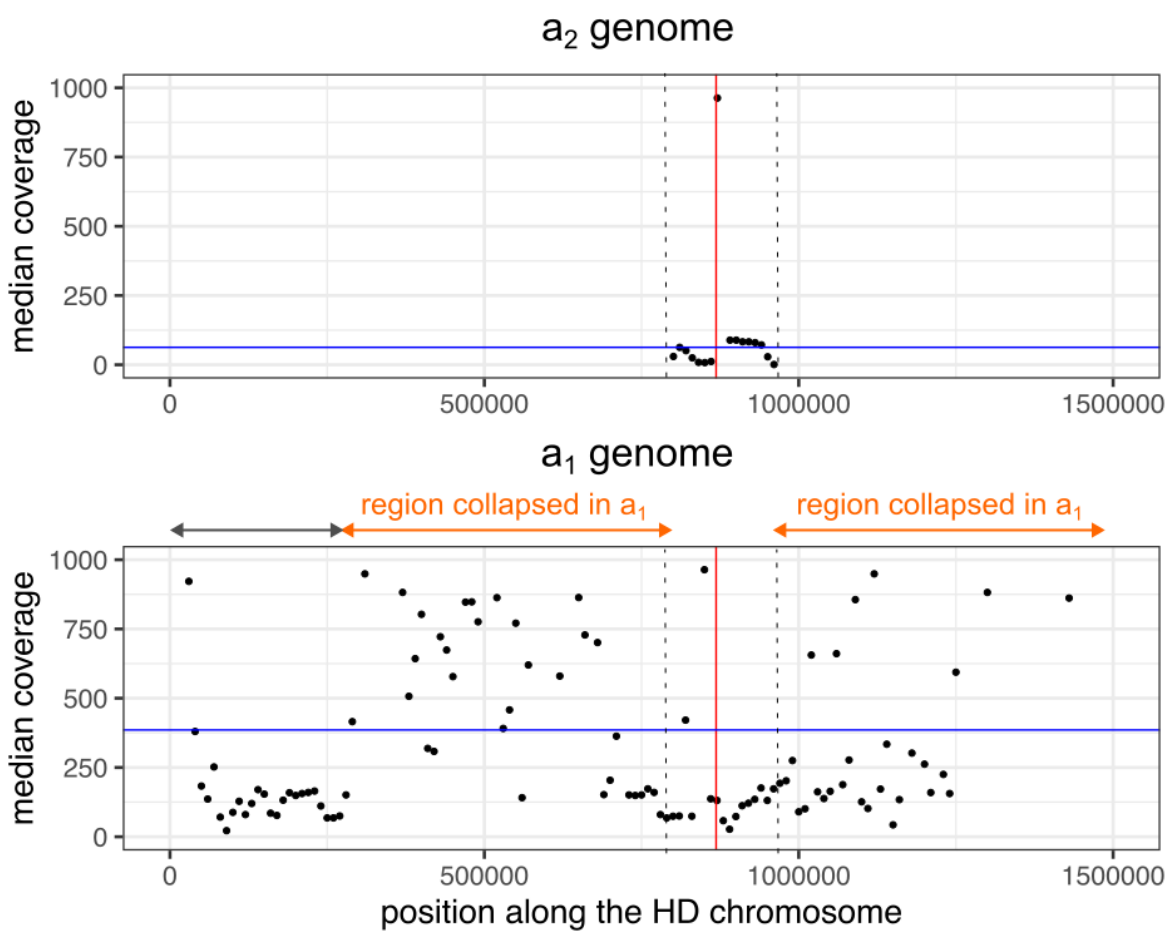

1426 **Figure S8: Read mapping coverage along the HD chromosome in *Microbotryum shykoffianum*.**
1427 The mapping coverage is represented against the a_2 genome at the top and against the a_1 genome at the
1428 bottom. The location of the canonical HD mating-type genes is represented by the red vertical bar. The
1429 median read coverage is indicated by the blue horizontal bar. The orange arrows represent the regions
1430 collapsed in the a_1 genome assembly. The region delimited by vertical dotted lines is the region that
1431 was assigned correctly to a_1 and a_2 mating types. The grey arrow represents a region that might be
1432 missing from the a_2 genome.

1433

1434

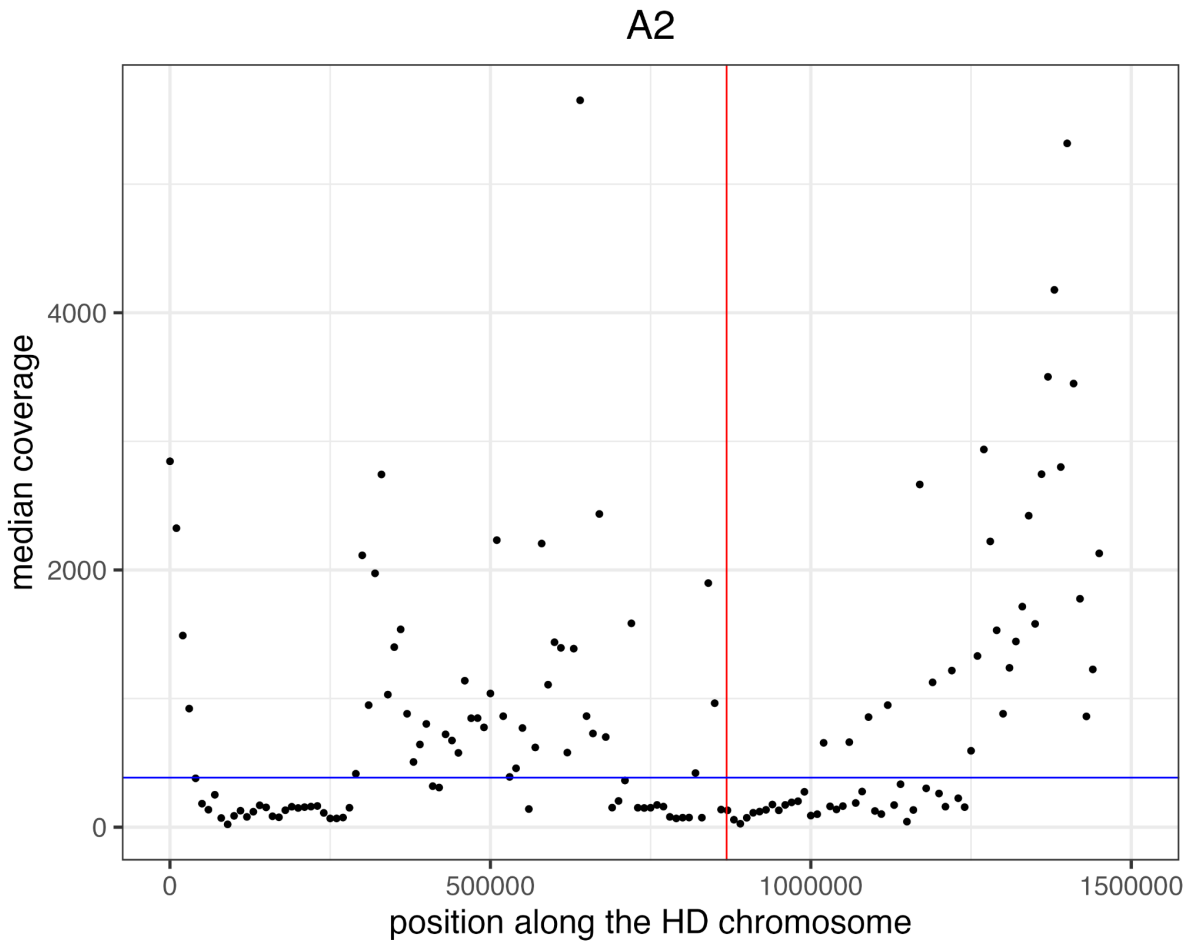
A2
median coverage
4000
2000
0
0
500000
1000000
1500000
position along the HD chromosome

1435

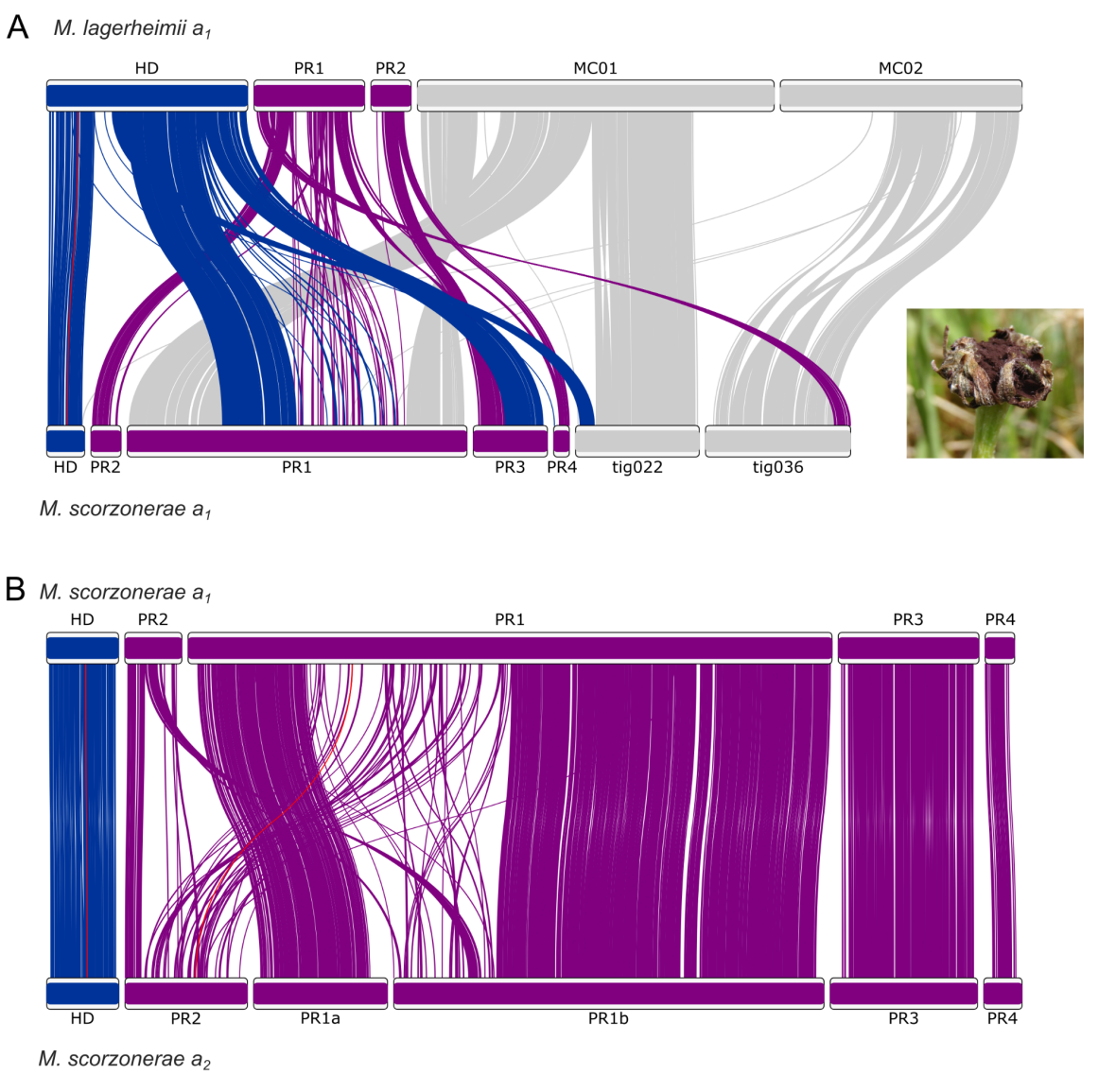

1436 **Figure S9: Synteny and rearrangements between the a_1 genomes of *Microbotryum scorzonarae***
1437 **and *M. lagerheimii* (A) and between a_1 and a_2 genomes of *M. scorzonarae* (B).** The *M. lagerheimii*
1438 genome represents a proxy for the ancestral state. The HD and PR loci are linked between genomes by
1439 red links. On the right, a picture of a diseased flower.

1440

1441

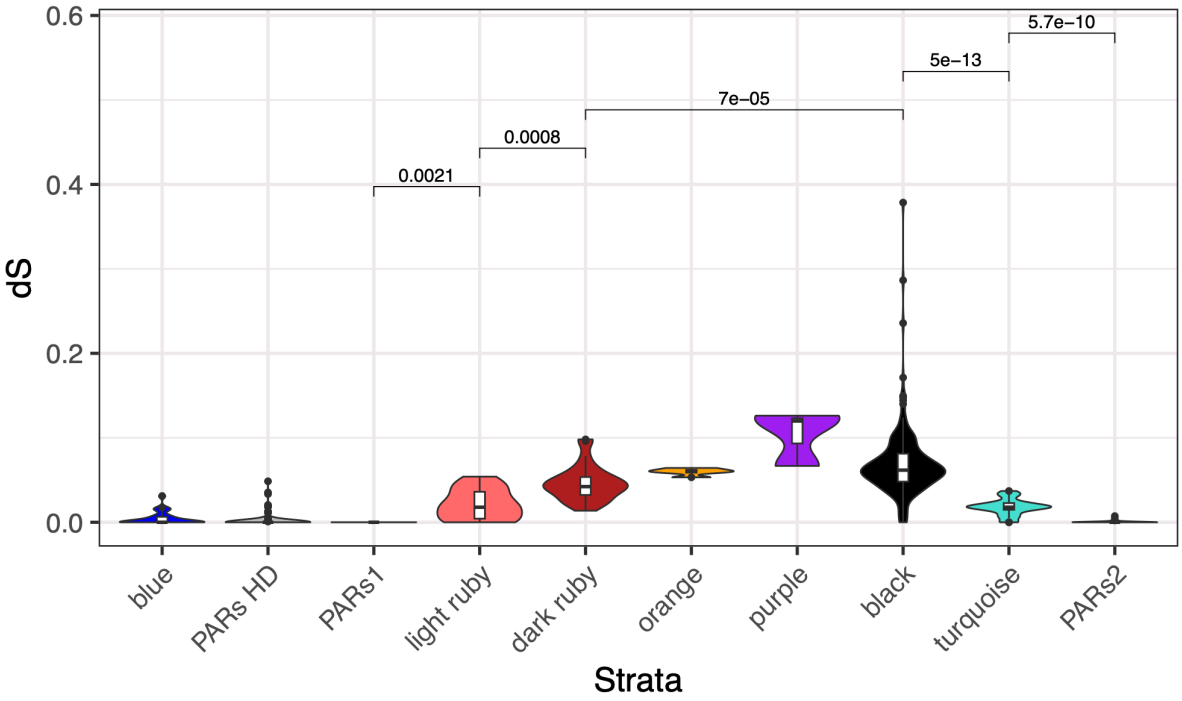

1442 **Figure S10:** Boxplot of the synonymous divergence (d_S) values for each stratum in *Microbotryum*
1443 *superbum*. Wilcoxon tests were performed between each pairwise comparison of strata to assess
1444 significant differences in mean d_S between strata. Only significant p-values are shown.
1445

1446

1447

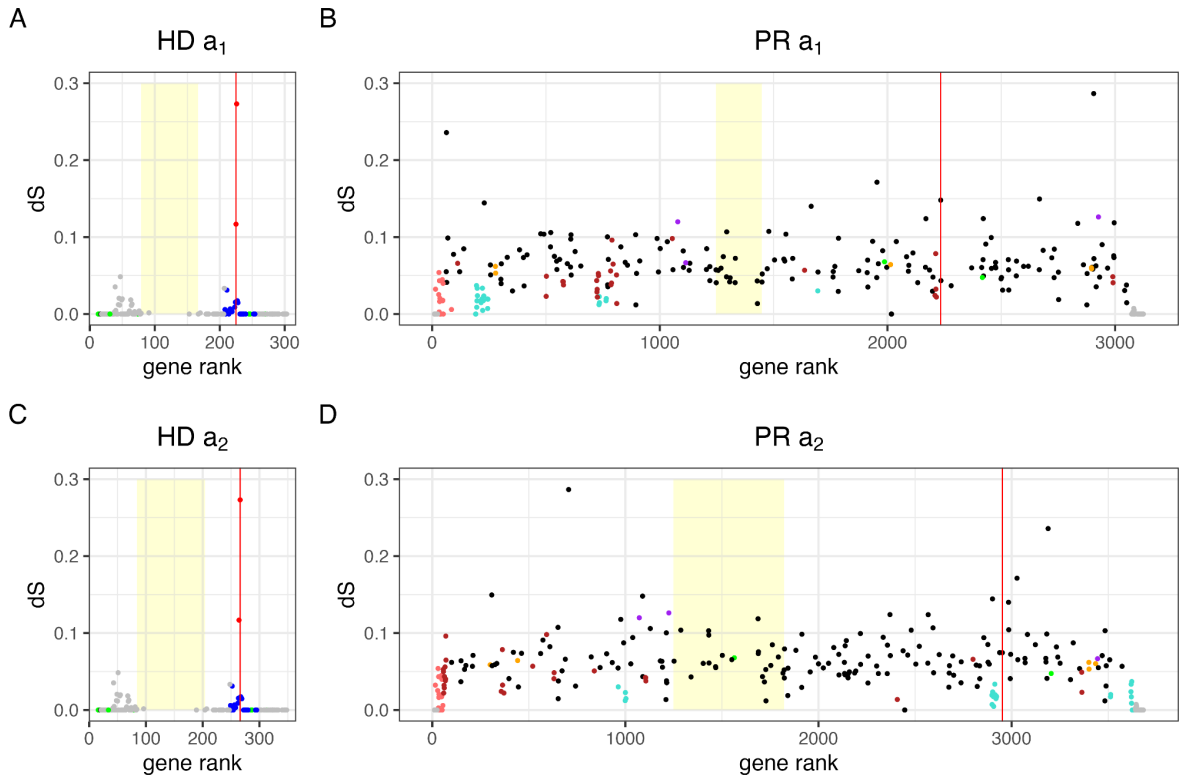

1448

1449 **Figure S11: Differentiation and rearrangements in the HD (A-C) and PR (B-D) mating-type**
1450 **chromosomes in *Microbotryum superbum*.** A-B correspond to the a_1 mating type, and C-D to the a_2
1451 mating type. Per-gene synonymous divergence (d_S) plotted along the current gene order in the PR and
1452 HD chromosomes, in the a_1 and a_2 genomes; the points are colored according to their evolutionary
1453 stratum assignment: turquoise, light ruby for the *M. superbum* specific evolutionary strata, dark ruby
1454 and black for the evolutionary stratum shared by *M. superbum* and *M. shykoffianum,* blue, orange and
1455 purple for the ancient evolutionary strata shared by most *Microbotryum* species. The pseudo-autosomal
1456 regions (PARs) are in grey. The genes ancestrally located in the alternative mating-type chromosome
1457 are in green (i.e. the genes ancestrally in the HD chromosome arm are in green on the PR chromosome,
1458 and reciprocally). The yellow boxes correspond to the position of the centromeres. The vertical red lines
1459 indicate the position of the HD and PR loci.

1460

1461

1462

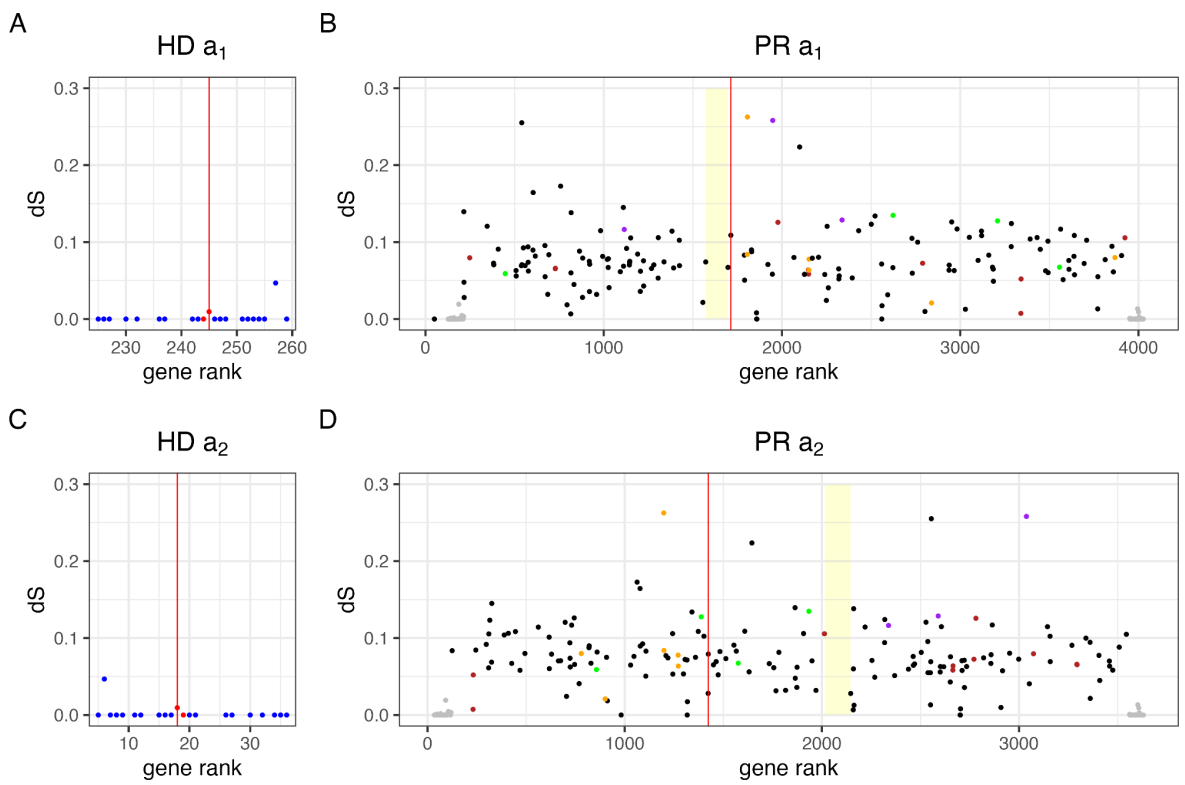

1463 **Figure S12: Differentiation and rearrangements in the HD (A-C) and PR (B-D) mating-type**
1464 **chromosomes in *Microbotryum shykoffianum*.** A-B correspond to the a_1 mating type, and C-D to the
1465 a_2 mating type. Per-gene synonymous divergence (d_S) plotted along the current gene order in the PR
1466 and HD chromosomes, in the a_1 and a_2 genomes; the points are colored according to their evolutionary
1467 stratum assignment: dark ruby and black for the evolutionary strata shared by *M. superbum* and *M.*
1468 *shykoffianum,* blue, orange and purple for the ancient evolutionary strata shared by most *Microbotryum*
1469 species. The pseudo-autosomal regions (PARs) are in grey. The genes ancestrally located in the
1470 alternative mating-type chromosome are in green (i.e. the genes ancestrally in the HD chromosome arm
1471 are in green on the PR chromosome, and reciprocally).

1472

1473

1474

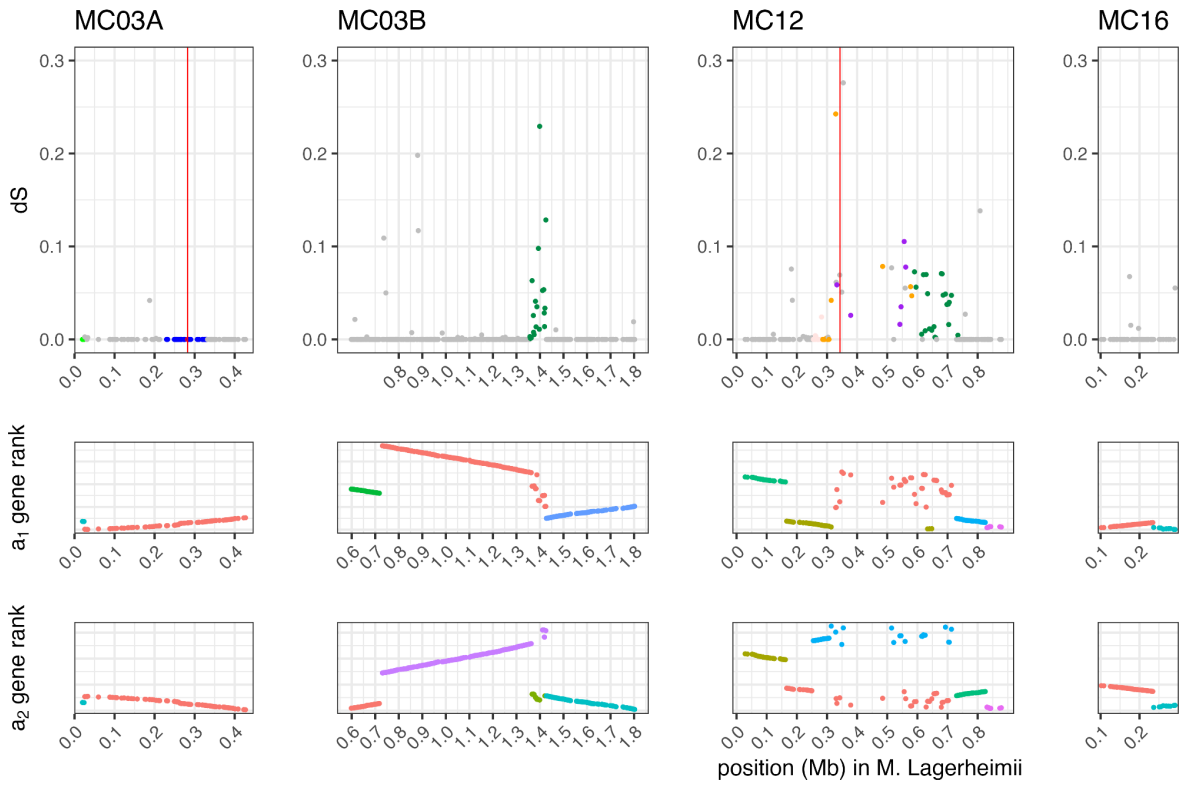

1475 **Figure S13: Differentiation and rearrangements between mating-type chromosomes in**
1476 ***Microbotryum scorzoraneae*. a)** Per-gene synonymous divergence (d_S) plotted along the ancestral gene
1477 order (taking as proxy the gene order along the *M. lagerheimii* mating-type chromosomes, its HD
1478 chromosomes encompassing the MC03A and B contigs and the PR chromosome the MC12 and MC16
1479 contigs). The points are colored according to their evolutionary stratum assignment: emerald and quartz
1480 for the young evolutionary stratum specific to *M. scorzonareae,* and blue, orange and purple for the
1481 ancient evolutionary strata shared by most *Microbotryum* species. The pseudo-autosomal regions
1482 (PARs) are in grey. **B)** Rearrangements compared to the ancestral gene order figured by plotting the
1483 gene rank in the current gene order (in the a_1 genome and in the a_2 genome) as a function of the gene
1484 rank in the ancestral gene order. The different contigs in *M. scorzonareae* have different colors in the
1485 gene rank panels.

1486

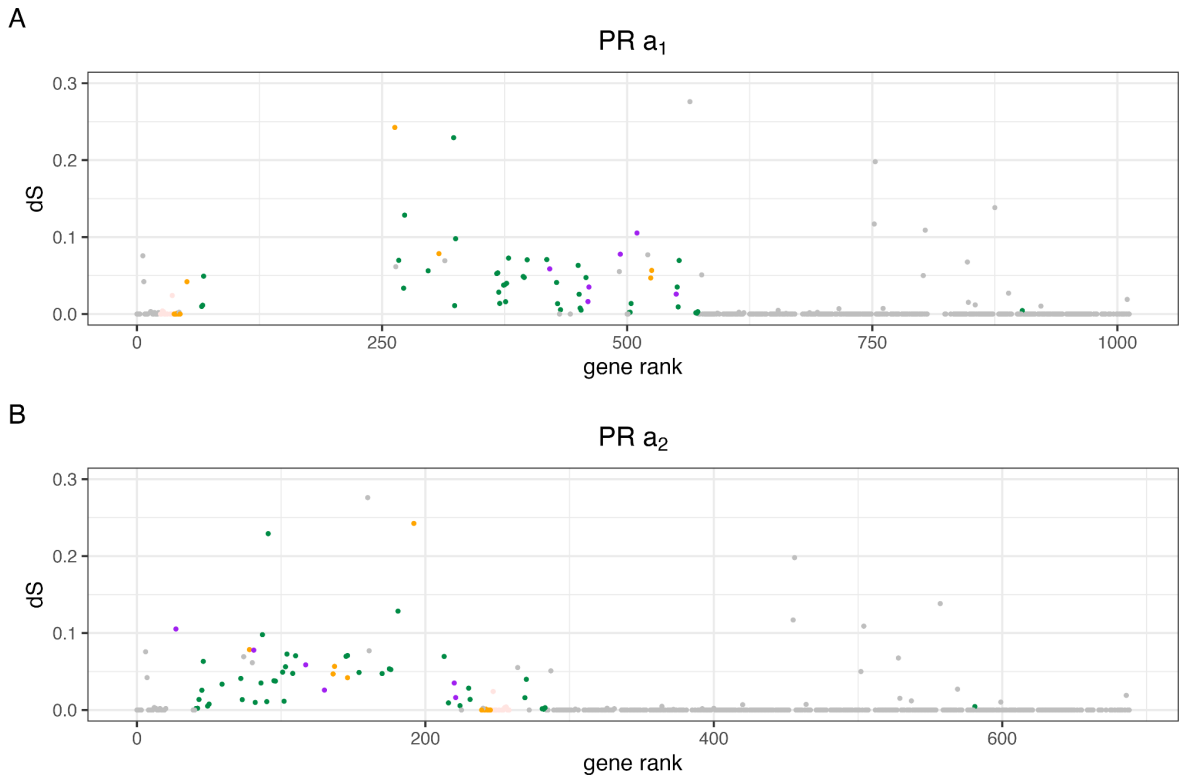

1487

1488 **Figure S14- Differentiation and rearrangements in the PR mating-type chromosomes in**
1489 ***Microbotryum scorzoraneae*.** Per-gene synonymous divergence (d_S) plotted along the current gene
1490 order in the PR chromosome in the a_1 (A) and a_2 (B) genomes; the points are colored according to their
1491 evolutionary stratum assignment: emerald and quartz rose or the *M. scorzoraneae* specific evolutionary
1492 strata, orange and purple for the ancient evolutionary strata shared by most *Microbotryum* species. The
1493 pseudo-autosomal regions (PARs) are in grey.

1494

1495

1496
1497

1498 **Supplementary Tables**

1499

1500

1501

Gene	Allele	Primer Forward	Primer Reverse
HD1	a_1	CCAAAGACGTGGCTGACTTC	ACCAGATGTCAGGACCGAAG
HD1	a_2	TGGAATCAAGCGAGCTGGTA	ATGTGGCGAGCGATGATGA
HD2	a_1	TGAGAGTGTCTTAAGCAGCCT	TTCTTCTTCCGTGCTAGCCA
HD2	a_2	CTCGAAACACTGCATTCCGT	AAGTCGGTAGGGTTGAACGA
PR	a_1	CTCTCGTCGACATCCCTCTC	CCGCCCAGTGACGATATACT
PR	a_2	CGACATAGGCGCAACTTTCA	AAGGCCGCAAAGAATACGAC

1502 **Table S1:** Primer pairs designed for specifically amplifying the different alleles at the genes HD1, HD2
1503 and PR as designed from *Microbotryum superbum* 1065.

1504

1505

1506

1507

1508

1509

1510

1511

1512

1513

1514
1515

1516

1517

Tetrad	Cell in tetrad	PR a_1	PR a_2	HD1 a_1	HD1 a_2	HD2 a_1	HD2 a_2
12	P	+	-	-	+	-	+
12	D	-	+	-	+	-	+
14	P	-	+	+	-	+	-
14	D	+	-	-	+	-	+
6	P	-	+	-	+	-	-
6	D	+	-	-	+	-	-
10	P	+	-	+	-	+	-
10	D	-	+	+	-	+	-
6	P	-	+	-	+	-	+
6	D	+	-	-	+	-	+
3	P	+	-	+	-	+	-
3	D	-	+	-	+	-	+

1518

1519 **Table S2:** Segregation of mating-type alleles in six tetrads of *Microbotryum superbum* (two opposite
1520 cells in a linear tetrad were analysed, i.e. P and D, corresponding to segregation at first meiotic division).
1521 A + sign indicates amplification by PCR of a fragment using primers designed to amplify specifically
1522 the a_1 or a_2 alleles in the *M. superbum* reference genome for the three mating-type genes PR, HD1 and
1523 HD2.

1524 **Table S3:** RNA seq sources (see excel file)

1525

1526